Renewable and Sustainable Energy Reviews 188 (2023) 113806

Contents lists available at ScienceDirect

Renewable and Sustainable Energy Reviews

journal homepage: www.elsevier.com/locate/rser

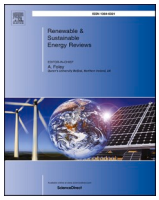

Hunting sustainable refrigerants fulfilling technical, environmental, safety and economic requirements

C.G. Albà [a,b], I.I.I. Alkhatib [a], F. Llovell [b,**], L.F. Vega [a,*]

[a] Research and Innovation Center on CO2 and Hydrogen (RICH Center) and Chemical Engineering Department, Khalifa University, PO Box 127788, Abu Dhabi, United Arab Emirates

[b] Department of Chemical Engineering, ETSEQ, Universitat Rovira I Virgili (URV), Campus Sescelades, Av. Països Catalans 26, 43007, Tarragona, Spain

ARTICLE INFO

Keywords:
Synthetic refrigerant blend
Polar soft-SAFT
Drop-in replacement
Low-GWP refrigerant
Regional environmental impact
Techno-economic analysis

ABSTRACT

An urgent action to mitigate climate change is the replacement of hydrofluorocarbons used in refrigeration systems, for low-global warming potential (GWP) alternatives, with stringent legislations in place. However, very limited options exist for single-component low-GWP refrigerants with similar technical performance. This work presents an integrated approach for the rational design of low-GWP refrigerant blends, focused on replacing R134a (GWP 1430), and R410A (GWP 2088), used in automotive and domestic air-conditioning, and in high pressure commercial and industrial refrigeration, respectively. A 4 E analysis (energy, exergy, economic and environmental) was employed to select suitable candidates. The molecular polar soft-SAFT theory was used in a predictive manner to fill the gap in thermodynamic data required for evaluating the technical performance based on initial selection criteria including GWP, toxicity, flammability, and degree of azeotropy. Potential candidates from a pool of 432 options were narrowed down and evaluated using a drop-in analysis to replace the working fluids R134a and R410A in today's refrigeration and air conditioning cycles, resulting in seven promising blends. Environmental and cost rate evaluation (geographically dependent based on electricity cost, HFC utilization taxes, and carbon emission factors) quantified the impact associated with their use and emissions, allowing to identify suitable replacements: three blends for replacing R134a: (90/10) *wt.*% R1243yf + R152a, (90/10) *wt.*% R1243yf + R134a, and (60/40) *wt.*% R1243zf + R1234ze(E), and one for replacing R410A: (90/10) *wt.*% R1123 + R32. This work showcases the importance of using robust thermodynamic models in the search of low-GWP refrigerants blends, considering the 4 E criteria.

1. Introduction

Climate change is one of the major environmental issues of the 21st century resulting from the atmospheric emissions of anthropogenic greenhouse gases (GHGs). With its recognized severity and need for immediate solutions, several countries worldwide have pledged net-zero emissions policies by 2050 [1,2]. Different alternatives to reduce atmospheric GHGs emissions have been proposed, including low to zero carbon energy sources, design of low emitting alternative novel processes, and capturing and utilizing or sequestering the produced CO_2, while new clean energy technologies take off [3].

Among the emitted GHGs, fluorinated compounds such as hydrofluorocarbons (HFCs), used in refrigeration and cooling systems, are targeted for immediate phase-out due to mandatory environmental regulations to mitigate climate change [4,5]. Although their atmospheric levels are substantially lower than CO_2, (*i.e.,* 237 ppt for HFCs *vs.* 410 ppm for CO_2 in 2019) [6], they significantly contribute to climate change due to their high global warming potential (GWP), 10–10,000 times higher than CO_2. HFCs emissions originate from their use as working fluids in commercial refrigeration and air conditioning circuits (RAC), and heating equipment, following the ban from the Montreal Protocol on the high ozone depleting predecessors, chlorofluorocarbons (CFCs) and hydrochlorofluorocarbons (HCFCs). Recently, with the implementation of Kigali's Amendment [5], the majority of global long-term initiatives on HFCs phase-out have become a reality. The European Union (EU) legislation (EU No. 517/2014) [4] enforced a ban on the commercial marketing of refrigerants with GWP >2500 in 2020, with a more stringent limit on GWP <150 in 2022, targeting an 80–95 % reduction of HFCs emissions by 2050 [7,8]. Concurrently, other regional

* Corresponding author.
** Corresponding author.
E-mail addresses: felix.llovell@urv.cat (F. Llovell), lourdes.vega@ku.ac.ae (L.F. Vega).

https://doi.org/10.1016/j.rser.2023.113806
Received 14 January 2023; Received in revised form 8 September 2023; Accepted 1 October 2023
Available online 14 October 2023

List of nomenclature

Abbreviations

AAD	Absolute Average Deviation
AOT	Operational hours in a year
AUT	Austria
BEL	Belgium
BUG	Bulgaria
CCUS	Carbon Capture, Utilization and Storage
CFC	ChloroFluoroCarbons
COP	Coefficient of Performance
COP_{Carnot}	Cycle's effectiveness in reversible conditions
CRF	Capital Recovery Factor
CYP	Cyprus
CZE	Czech Republic
DEU	Germany
DLT	Discharge Line Temperature (K)
DNK	Denmark
EEV	Electronic Expansion Valve
EoS	Equation of State
EST	Estonia
ESP	Spain
EU	European Union
EU-ETS	European Union-Emissions Trading System
FIN	Finland
FRA	France
GHG	GreenHouse Gases
GRC	Greece
GWP	Global warming potential
HCFC	HydroChloroFluoroCarbons
HCFO	HydroChloroFluoroOlefins
HFC	HydroFluoroCarbons
HFO	HydroFluoroOlefins
HOC	Heat of Combustion ($kJ \cdot kg^{-1}$)
HP	High Pressure side
HRV	Croatia
HUN	Hungary
JPN	Japan
IND	India
IRL	Ireland
ITA	Italy
LFL	Lower Flammability Level ($g \cdot m^{-3}$)
LJ	Lennard-Jones
LP	Low Pressure side
LTU	Lithuania
LVA	Latvia
LUX	Luxembourg
MLT	Malta
NBP	Normal Boiling Point (K)
NLD	The Netherlands
ODP	Ozone Depleting Potential
PH	Pressure-Enthalpy
POL	Poland
PPTD	Pinch Point Temperature Difference (K)
PPTR	Power Per Ton of Refrigeration ($kW \cdot TR^{-1}$)
PRC	People's Republic of China
PRT	Portugal
ROU	Romania
RE	Refrigeration Effect ($kJ \cdot kg^{-1}$)
SAFT	Statistical Associating Fluid Theory
SC	SubCooling degree (K)
SH	Superheating degree (K)
Soft-SAFT	soft-Statistical Associating Fluid Theory
SS-VCRC	Simple System
SVK	Slovakia
SVN	Slovenia
SWE	Sweden
TAC	Total Annualized Cost ($\$.y^{-1}$)
TEWI	Total Equivalent Warming Impact (tCO_2-eq)
TS	Temperature-Entropy
VCC	Volumetric Cooling Capacity ($kJ \cdot L^{-1}$)
USA	United States of America
VCRC	Vapor Compression Refrigeration Cycle
VLE	Vapor-Liquid Equilibria

Notations and Symbols

A	Heat transfer area (m^2)
$\dot{C}$	Total cost rate ($US\$ \cdot y^{-1}$)
c_{CO_2}	Unit cost of CO_2 avoided ($US\$ \cdot kgCO_2\text{-eq}^{-1}$)
$\dot{C_{env}}$	Penalty cost rate of CO_2 emissions ($US\$ \cdot y^{-1}$)
$\dot{C_{op}}$	Operational cost rate ($US\$ \cdot y^{-1}$)
$\sum \dot{C_k}$	Capital and maintenance cost rate ($US\$ \cdot y^{-1}$)
C_{set-up}	Set-up cost (US$)
E_a	Yearly energy consumption (kWh)
$\left(\frac{F}{F+H}\right)$	Ratio of fluorine atoms to the total number of fluorine and hydrogen atoms
H	Specific enthalpy ($kJ \cdot kg^{-1}$)
i	Annual interest rate
L	Annual leakage rate
m	Refrigerant charge load (kg)
m_i	Chain length
$\dot{m}$	Mass flow rate ($kg \cdot s^{-1}$)
m'	Total amount of refrigerant used throughout the system lifecycle (kg)
$m_{CO_2,e}$	Annual greenhouse gas emissions ($kgCO_2\text{-eq} \cdot y^{-1}$)
n	System lifetime (y)
P_{atm}	Atmospheric Pressure (MPa)
P_{cond}	Condenser Pressure (MPa)
P_{ev}	Evaporator Pressure (MPa)
P_R	Pressure Ratio
RP	Retail price ($US\$ \cdot kg^{-1}$)
$\dot{Q}$	Heat flow (kW)
$\dot{Q_{cond}}$	Heating capacity (kW)
$\dot{Q_{ev}}$	Cooling capacity (kW)
S	Specific entropy ($kJ \cdot kg^{-1} \cdot K^{-1}$)
T_0	Dead-state temperature (K)
T_{ad}	Adiabatic flame Temperature (K)
$\overline{T}_C$	Evaporator entropy-averaged temperature of the auxiliary fluid (K)
$\overline{T}_H$	Condenser entropy-averaged temperature of the auxiliary fluid (K)
Tax_{CO_2}	CO_2 tax ($US\$ \cdot tCO_2\text{-eq}^{-1}$)
Tax_{HFC}	HFC tax ($US\$ \cdot kg^{-1}$)
$T_{c,in}$	Temperature of auxiliary fluid entering the condenser (K)
$T_{c,out}$	Temperature of auxiliary fluid departing the condenser (K)
$T_{cond,in}$	Condenser inlet temperature (K)
$T_{cond,out}$	Condenser outlet temperature (K)
$T_{ev,in}$	Evaporator inlet temperature (K)
$T_{ev,out}$	Evaporator outlet temperature (K)
T_G	Glide Temperature (K)
$T_{h,in}$	Temperature of auxiliary fluid entering the evaporator (K)
$T_{h,out}$	Temperature of auxiliary fluid departing the evaporator (K)
T_L	Evaporator boundary Temperature (K)
U	Overall heat transfer coefficient ($W \cdot m^{-2} \cdot K^{-1}$)
$\dot{W}$	Compressor power (kW)
wt.%	Weigh percentage
x_p	Fraction of dipolar segment
α	Recovery factor

α_{el}	Unit electricity cost (US$·kWh^{-1})	ρ_V	Suction density (mol·L^{-1})
β	Indirect emission factor (kgCO_2-eq·kWh^{-1})	σ_i	Segment diameter (Å) parameter in the soft-SAFT equation
ε	Intercooler effectiveness	φ	Maintenance factor
ε_i/k_B	Dispersive energy (K) parameter in the soft-SAFT equation	ψ	Specific exergy (kJ·kg^{-1})
η_{is}	Compressor isentropic efficiency	ω_{comp}	Net cycle compressor's work (kJ·kg^{-1})
η_{II}	Second law efficiency	$\dot{\chi}$	Physical Exergy (kW)
η_{ij}	Adjustable size binary parameter	$\dot{\chi}_d$	Exergy Destruction (kW)
μ	Experimental dipole moment (C·m)	$\dot{\chi}_{d,i}$	Exergy Destruction of component i (kW)
ξ_{ij}	Adjustable energy binary parameter		
$\overline{\Pi}$	Normalized flammability index		

initiatives have been implemented, such as developing green technologies, HFCs utilization taxes, and HFCs allowance allocation and trading programs [9–11].

Thus far, the complete removal of HFCs from market circulation is imminently close, begging an immediate answer to the elusive question *"what are the alternative sustainable refrigerants replacing the technically efficient HFCs?"* The National Institute of Standards and Technology (NIST) developed a framework to investigate new classes of potential refrigerants meeting imposed environmental and safety regulations, and maintaining technical efficiencies of widely used high-GWP HFCs such as 1,1,1,2-tetrafluoroethane (R134a) and R410A (blend of difluoromethane (R32) + pentafluoroethane (R125)) [12]. From a pool of 56,000 single-component refrigerants, limited options for low GWP refrigerants existed, with 27 potential candidates balancing environmental, safety, and technical trade-offs, mainly from hydrofluoroolefins (HFOs) [13]. Additional investigations on the operational compatibility of pure 4th generation refrigerants HFOs and hydrochlorofluoroolefins (HCFOs) as drop-in replacements (*i.e.,* with minimal modifications to existing systems) identified their potential to only replace a small pool of commercial single-component HFCs (*e.g.,* R134a, 1,1-difluoroethane (R152a), and 1,1,1,3,3-pentafluoropropane (R245fa)), with no viable replacements for the majority of widely used HFCs [14]. Moreover, the most promising HFOs such as, 2,3,3,3-tetrafluoroprop-1-ene (R1234yf) and *trans*-1,3,3,3-tetrafluoroprop-1-ene (R1234ze(E)), are mildly-flammable (A2L ASHRAE classification) [15] compared to non-flammable HFCs in use (A1 class) [15] R134a and R410A, which might be reflected on the costs required for additional safety layers [16,17]. Though several low GWP refrigerants have been recently identified [7,17–19], their market deployment is constrained by several barriers in global and country-specific contexts, spanning across (1) technical barriers of safety-related properties and limited range of applications, (2) technological barriers related to high investment costs either for retrofitting existing systems or deploying newly designed systems with low GWP refrigerants, and (3) commercial barriers associated with misaligned commercial interests of industrial sectors with imposed regulations [20–23].

Refrigerant blends are promising alternatives that can circumvent existing barriers towards deployment of low GWP refrigerants, with a summary of promising replacements that are ready for commercialization based on GWP <600 listed in Table 1. This is attributed to the additional degrees of freedom during blend design, facilitating a targeted fine-tuning of blend properties within environmental/safety constraints and technical requirements. The use of refrigerant blends is not uncommon, as seen with the release of R410A with the phase-out of chlorodifluoromethane (R22) and dichlorodifluoromethane (R12) [24,25]. Similarly, synthetic medium-GWP blends (*i.e.,* GWP ≈ 500–750) exploiting low-GWP HFOs and non-flammable HFCs [26] such as R513A and R450A, have been proposed as mid-term replacements for R134a (GWP = 1300), given their high technical performance [27,28]. Nonetheless, their adequacy has to be re-evaluated with the realigned GWP constraints [4], hence, the need for alternative low-GWP synthetic blends.

For promising drop-in replacement blends, the same criteria for single-component candidates applies, wherein the blend should: (1) minimize GWP, (2) minimize/eliminate flammability, (3) be non-toxic and have null ozone depleting potential (ODP), (4) maximize/

Table 1
Summary of alternative drop-in replacement blends, specifying their proportion, GWP, normal boiling point (NBP) and glide temperature (T_G).

Blend	*wt.%*	GWP	ASHRAE Class	*NBP* (°C)	T_G (K)	Baseline	Ref.
R1234ze(E) + R152a	10/90	112.2	A2	−24.41	0.013	R134a/R410A	[29,30]
R600a + R1234ze(Z)	90/10	18.6	A3	−11.77	0.001	R134a/R410A	[29]
R600a + R1233zd(E)	90/10	31.4	A3	−11.92	0.031	R134a/R410A	[29]
R450A (R1234ze(E) + R134a)	58/42	547	A1	−23.36	0.640	R134a	[29,31–33]
R513A (R1234yf + R134a)	56/44	573	A1	−29.58	0.000	R134a	[31]
R1234ze + R134a	90/10	150	A2L	−21.40	0.930	R134a	[34,35]
R430A (R152a + R600a)	76/24	107	A3	−27.60	0.200	R134a	[36]
R431A (R290 + R152a)	71/29	43	A3	−43.20	0.000	R134a	[36]
R435A (RE170 +R152a)	80/20	30	A3	−26.00	0.200	R134a	[36]
R436A (R290 + R600a)	56/44	<3	A3	−34.30	8.200	R134a	[36]
R600a + R1224yd(Z)	90/10	18.1	A2L – A3	−12.03	0.081	R134a/R410A	[29]
R1243zf + R152a	10/90	111.7	A2	−24.88	0.103	R134a/R410A	[29]
R600a + R236ea	90/10	138	A2L – A3	−12.18	0.217	R134a/R410A	[29]
R1234yf + R152a	10/90	112	A2L – A2	−25.13	0.236	R134a/R410A	[29,35]
R600a + R245fa	90/10	121	A3	−12.97	0.756	R134a/R410A	[29]
R152a + R600	90/10	99.8	A2	−25.92	0.194	R134a/R410A	[29]
R454A (R32 + R1234yf)	35/65	238	A2L	−47.80	5.000	R404A	[37,38]
R454C (R32 + R1234yf)	21.5/78.5	146	A2L	−45.50	6.000	R404A	[37–39]
R32 + R1234yf + R744	22/72/6	149	A2L	−57.50	14.120	R410A	[40]
R455A (R744 + R32 +R1234yf)	3/21.5/75.5	146	A2L	−52.00	9.860	R404A	[38,39]
R457A (R32 + R1234yf + R152a)	18/70/12	139	A2L	−42.60	6.140	R404A	[39]
R459B (R32 +R1234yf + R1234ze(E))	21/69/10	143	A2L	−45.00	7.040	R404A	[39]

*R600 (*n*-butane), R600a (*i*-butane), R774 (CO_2), RE170 (Dimethyl ether).

maintain circuit efficiency, and (5) possess equivalent volumetric cooling capacity (VCC) to ensure minimal retrofitting to key cooling cycle units, such as the compressor [41]. Accordingly, a drop-in replacement has to meet imposed environmental and safety regulations and ensure meeting technical specifications that can maintain or further enhance the system efficiency, which in turn is reflected on the energy consumption and environmental footprint. This is a complex task for single-component refrigerants considering the trade-offs between the multiple desirable properties, becoming more complicated for blends as their appropriate individual constituents and proportions must be determined. An additional selection criterion for blends is their degree of azeotropy, with preference for azeotropic or near-azeotropic blends that behave as pure fluids in the cooling system. Although zeotropic blends can be used, such as the ternary mixtures R407C (blend of R32 + R125 + R134a) and R404A (blend of R125 + R134 + (1,1,1-trifluoroethane) R143a), several operational challenges arise, including glitches through refrigerant charging, flooded evaporators, blend composition shifts during leakages, lower heat transfer efficiency, and lower overall efficiency [38,42,43]. Fully azeotropic blends are very limited, with only 17 mixtures registered and classified in the R500 series, part of which have either high-ODP or high-GWP [44]. Consequently, developing alternative near-azeotropic blends is more flexible [45].

Indeed, the design of blends is a daunting task considering the multiple desirable properties and range of possible blend constituents and proportions suitable for a specific application, requiring detailed knowledge of their thermodynamic properties [43,46]. A recent survey of experimental data for refrigerant blends containing 4th generation refrigerants noted the sparsity in measured properties due to the taxing nature of experimental investigations, hindering their detailed technical evaluation [47].

Computational modeling tools can be pragmatically employed for the rational design of refrigerant blends under imposed environmental and technical constraints [43,48–50]. With these tools, a multitude of possible blends can be rapidly and efficiently screened with minimal need for experimental data, while being sufficiently flexible to examine diverse ranges of applications and amendments in environmental legislations. However, the developed screening framework would be as reliable as the chosen thermodynamic model, with a broad spectrum of available models such as empirical correlations, classical cubic equations of state (cEoSs), and advanced molecular-based EoSs [51]. Mickoleit et al. [51], examined the effect of thermodynamic models on parameters of interest for the design of refrigeration processes, highlighting the impact of the chosen model on the predicted performance parameters, and subsequently, conclusions on the technical adequacy of the working fluid. A review by Bell et al. [47] noted the adequacy of NIST's REFPROP semi-empirical model [52] for engineering applications, however, raising concerns on its predictive accuracy, parameters transferability, and extensive need for experimental data for new blends.

Concurrently, molecular-based EoSs formulated based on the Statistical Associating Fluid Theory (SAFT) [53] have demonstrated success in accurately predicting thermodynamic properties of 3rd and 4th generation refrigerants, providing an attractive tool for the rational design of refrigerant blends [54–67]. This is attributed to their ability to explicitly account for micro-level characteristics (*i.e.,* molecular structure, and intermolecular interactions) and their impact on observable macro-level phenomena. The accuracy and predictive capabilities of the polar soft-SAFT EoS [68,69] in characterizing the thermodynamic behavior of pure 3rd and 4th generations refrigerants has been demonstrated in previous studies [14,70].

This research presents for the first time the application of polar soft-SAFT as a reliable platform to rationally design new low-GWP azeotropic/near-azeotropic refrigerant blends as drop-in replacements for the widely used commercial refrigerants R134a and R410A. The scope of this work is limited to binary blends with available phase equilibria experimental data to demonstrate the reliability of the model and proposed blend design framework. A total of 48 blends of binary mixtures composed of HFCs + HFCs, HFCs + HFOs, HFOs + HFOs, and HFOs + HCFOs were evaluated using the molecular modeling tool. Once the validity of the model against experimental data was established, an initial screening was performed to narrow-down possible blend combinations and proportions, focusing on non-toxic and low-GWP blends with near-azeotropic behavior and non-to mild-flammability. Subsequently, shortlisted potential blends were evaluated for their technical compatibility as drop-in replacements to R134a and R410A in a simple refrigeration cycle based on selected key performance indicators (KPIs) to ensure minimal system retrofitting. The evaluation of the promising blends was concluded with a 4 E analysis, examining their energetic and exergetic performance, environmental impact, and projected blends economics for a holistic view on the impact associated with their deployment as alternatives to those in current circulation. With this modeling approach, new alternative blends are designed meeting imposed environmental and safety regulations, while having better energetic, environmental, and economic impact compared to current systems using R134a and R410A for cooling applications.

2. Methodology

2.1. The polar soft-SAFT equation

In polar soft-SAFT the residual Helmholtz energy of a fluid (a^{res}) is calculated considering the different intra- and intermolecular features of the molecules comprising it, as:

$$a^{res} = a^{LJ} + a^{chain} + a^{assoc} + a^{polar} \tag{1}$$

with, a^{LJ} representing the Lennard-Jones (LJ) reference fluid segment-segment repulsive and attractive interactions of the groups forming the molecules, a^{chain} accounting for the formation of chains from connected segments, a^{assoc} denoting the contribution from hydrogen bonding or association, and a^{polar} accounting for the polar nature of the fluid. In this work, a^{assoc} is not considered, as refrigerants present a permanent dipole moment rather than hydrogen bonding.

The reference term is computed using Johnson's LJ EoS [71], while the expressions for the chain and association terms are those derived by Chapman et al. [72,73] from Wertheim's 1st order thermodynamic perturbation theory [74–77]. The polar term is based on the theory of Gubbins and Twu [78,79] for spherical molecules, and its extension to chainlike fluids using the segment-approach of Jog and Chapman [80,81], computing dipole-dipole, quadrupole-quadrupole, and dipole-quadrupole interactions in the Padé approximation [82], as:

$$a^{polar} = \frac{a_2^{polar}}{1 - a_3^{polar}/a_2^{polar}} \tag{2}$$

where a_2^{polar} and a_3^{polar}, are the second and third order perturbation terms, respectively, related to two-body and three-body interactions, with the pair- and triplet-integral correlation functions for the LJ reference fluid from Luckas et al. [83] Additional details on the expressions of the model can be found elsewhere [68,69,84–87].

The chain and polar terms are explicitly written for mixtures, while the generalized Lorentz-Berthelot combining rules are used to calculate the crossed energy, ε_{ij}, and size, σ_{ij} of the reference term for mixtures, as:

$$\varepsilon_{ij} = \xi_{ij}\sqrt{\varepsilon_{ii}\varepsilon_{jj}} \tag{3.a}$$

$$\sigma_{ij} = \eta_{ij}\frac{(\sigma_{ii} + \sigma_{jj})}{2} \tag{3.b}$$

where ξ_{ij} and η_{ij} are the adjustable energy and size binary parameters, respectively. Their values are fixed to unity when using the model in a predictive manner, otherwise they are regressed to binary mixture vapor-liquid equilibria (VLE) data.

To apply polar soft-SAFT to experimental systems, a molecular model

representative of key molecular features is required. Reliable molecular models for the ten HFCs, four HFOs, and HCFO included in this work, listed in Table 2, are used from previous works [14,88] (see Table S1 in the Supporting Information (SI)). Refrigerants were modeled as non-associating chainlike fluids with a chain length (m_i), segment diameter (σ_i), dispersive energy (ε_i), and a dipole moment (μ). The values of m_i, σ_i, ε_i were regressed using saturated liquid density and vapor pressure data of the pure refrigerants, while for the polar parameters the experimental dipole moment (μ) was used, as well as an *a priori* fixed fraction of dipolar segments (x_p), based on established procedures [69,84–86].

Thorough examination of available experimental VLE data for refrigerants binary blends of HFCs + HFCs, HFCs + HFOs, HFOs + HFOs, and HFOs + HCFOs comprised of the 15 refrigerants in Table 2, established data availability for 48 binary mixtures listed in Table 3.

The reliability of polar soft-SAFT for modeling refrigerant binary blends was validated by comparing the model performance to experimental data, needed to ensure high fidelity in the model's predictions for all thermodynamic state variables used in the technical evaluation of identified promising refrigerant blends. The phase equilibria of selected binary mixtures with R32, R134a, R1234yf, and R1234ze(E), depicted in Fig. 1, demonstrated the predictive accuracy of polar soft-SAFT from the highly precise correlations of experimental VLE data (see Table S2 in the SI for absolute average deviation (AAD) in % of selected binary mixtures) with minimal to no-calibration to the data, simply from the molecular parameters of the pure refrigerants. Similar plots are included in Fig. S1 in the SI. In the few cases where the model required calibration, temperature-independent binary energy parameters (ξ_{ij}) close to unity were fine-tuned to experimental VLE data by minimizing the AAD. This was needed to correct the crossed dispersive interactions between the individual components of the blend, on account of approximating their dipolar interactions rather than their explicit parametrization. Notwithstanding, the ξ_{ij} energy binary parameter, when needed, proved highly transferable as seen with blends of R1234ze(E) with R152a, R161, and R1243zf in Fig. 1d, modeled with the same binary parameter ($\xi_{ij} = 1.010$). These results ensure the reliability of the model as a platform for the rational design of refrigerant blends with highly accurate calculations deviating within 0.32–3.76 % from available VLE experimental data from Table S2 in the SI.

2.2. Initial screening criteria of near-azeotropic refrigerant blends

The proportions of the blends listed in Table 3 were examined in the composition range of 10–90 *wt*%, discretized with 10 *wt*%; resulting in 432 possible blends. An initial screening in Fig. 2 based on GWP, degree of azeotropy, toxicity, and flammability class was conducted to determine blends for further evaluation as potential drop-in replacements.

For the environmental criterion, the blend GWP was computed as the sum of the weighted average of the individual components' GWP [125]. The constraints on GWP were set to (1) GWP <150, termed study A, based on 2022 EU legislation limits [4], and (2) 150 < GWP <500, study B, emulating 2020 interim stage transitionary legislations [4]. For safety constraints, blends comprised of toxic components were eliminated, while those with flammable components (A2/A3) were still included, pending a flammability assessment dependent on their proportions, if satisfying remaining criteria.

The technical criteria on degree of azeotropy was evaluated based on the blend glide temperature (temperature variation between dew and bubble points at constant pressure and single-phase composition), obtained from VLE predictions for the binary blends using the molecular model. As highlighted earlier, blends with null (azeotropic) or small (near-azeotropic) glide temperatures are preferred, behaving as pure fluids in cooling systems. In this study, acceptable T_G was set to 0.1 K, benchmarked to the T_G of the near-azeotropic blend R410A at atmospheric pressure [126], although this criterion can be less stringent for other applications. This was used to the entire pressure spectra to ensure applicability within common industrial operating pressures (*i.e.,* 0.1–3 MPa), accounting for pressure fluctuations in system operations.

The flammability of the short-listed blends was evaluated using Linteris et al. [127] empirical approach. With this method a normalized flammability index ($\overline{\Pi}$) is estimated using the adiabatic flame temperature (T_{ad}), and degree of fluorination, expressed as the ratio of fluorine atoms to the total number of fluorine and hydrogen atoms ($\frac{F}{F+H}$). The values for the pure refrigerants were obtained from other studies [127–129], and used to predict the flammability class for the selected blends. The flammability class for blends in-line with the ASHRAE classification are grouped based on their $\overline{\Pi}$ values, with non-flammable class 1 ($\overline{\Pi} \leq 0$), mild-flammable class 2 L ($0 < \overline{\Pi} < 50$), and flammable classes 2 and 3 ($\overline{\Pi} \geq 50$), shortlisting blends with either 1 or 2 L flammability classes.

2.3. Technical evaluation of potential drop-in replacement blends based on key performance indicators

The short-listed refrigerant blends satisfying the initial screening criteria (**Section 2.2**) were evaluated based on their technical compatibility as drop-in replacements for R134a and R410A in a simple single-stage vapor compression refrigeration cycle (*SS*-VCRC), represented in Fig. 3a. The *SS*-VCRC operates with the non-isentropic compression of superheated vapor (85 %) in the single-stage reciprocating air compressor (1–2), followed by the isobaric de-superheating of the working fluid in a series of shell-and-tube air-to-refrigerant heat exchangers (2–2*). Condensation occurs afterward, releasing both its latent (2* – 3^{SAT}) and specific (3^{SAT} – 3) heats to deliver a subcooled liquid phase working fluid. This is followed by temperature and pressure reductions in the electronic expansion valve (EEV) (3–4), with the multiphase mixture cooling the high-temperature heat sink in the evaporator coil by releasing its latent and sensible heats, reaching a single-phase superheated vapor (4–1). Note that the temperature-entropy (*TS*) diagrams for near-azeotropic blends depicted in Fig. 3c account for their phase change (*i.e.,* evaporation and condensation) along their T_G rather than at constant temperature as with pure refrigerants and azeotropic blends. The assumptions for simulating *SS*-VCRC cycle include outlet evaporator temperature ($T_{ev} = T_1$) of 263.1 K, discharge condenser temperature ($T_{cond} = T_3$) of 293.1 K, isentropic compression, and zero pressure drop in the heat exchangers. As reflected in Fig. 3b–c, a 5 K superheating and subcooling were applied to lengthen the lifespan of the compressor and EEV. Simulations were performed

Table 2
Summary of the HFCs, HFOs, and HCFOs included in this work.

ASHRAE designation	IUPAC Name	ASHRAE designation	IUPAC Name
3rd gen. HFCs		**4th gen. HFOs**	
R41	Fluoromethane	**R1123**	1,1,2-trifluoroethene
R32	Difluoromethane	**R1243zf**	3,3,3-trifluoroprop-1-ene
R23	Trifluoromethane	**R1234yf**	2,3,3,3-tetrafluoroprop-1-ene
R161	1-fluoroethane	**R1234ze(E)**	*trans*-1,3,3,3-tetrafluoroprop-1-ene
R152a	1,1-difluoroethane	**4th gen. HCFOs**	
R134a	1,1,1,2-tetrafluoroethane	**R1233zd(E)**	*trans*-1-chloro-3,3,3-trifluoropropene
R125	1,1,1,2,2-pentafluoroethane		
R245fa	1,1,1,3,3-pentafluoropropane		
R236fa	1,1,1,3,33-hexafluoropropane		
R227ea	1,1,1,2,3,3-heptafluoropropane		

Table 3
The forty eight binary blends studied in this work with their experimental data, divided into HFCs + HFCs, HFCs + HFOs, and HFOs + HCFOs, and ξ fitted to experimental VLE data with η fixed to unity.

Mixture	ξ_{ij}	Ref.	Mixture	ξ_{ij}	Ref.	Mixture	ξ_{ij}	Ref.
HFCs + HFCs			**HFCs + HFOs**			**HFOs + HCFOs**		
R32 + R23	1.000	[89]	R41 + R1234yf	0.980	[90]	R1123 + R1234yf	1.000	[91]
R32 + R161	1.050	[92]	R32 + R1123	0.985	[91]	R1123 + R1234ze(E)	1.000	[91]
R32 + R152a	0.975	[93]	R32 + R1234yf	0.970	[94]	R1243zf + R1234ze(E)	1.010	[95]
R32 + R134a	0.980	[93]	R32+ R1234ze(E)	1.000	[96]	R1234yf + R1234ze(E)	1.000	[97]
R32 + R125	0.985	[93]	R23 + R1234yf	0.970	[98]	R1234yf + R1233zd(E)	0.990	[99]
R32 + R236fa	1.000	[100]	R161 + R1234yf	1.010	[94]			
R32 + R227ea	1.000	[101]	R161 + R1234ze(E)	1.010	[92]			
R23 + R152a	1.000	[102]	R152a + R1243zf	1.000	[103]			
R23 + R134a	1.000	[104]	R152a + R1234yf	0.980	[105]			
R23 + R125	0.975	[89]	R152a + R1234ze(E)	1.010	[106]			
R23 + R227ea	0.960	[107]	R134a + R1243zf	0.980	[108]			
R161 + R134a	1.045	[109]	R134a + R1234yf	0.983	[110]			
R161 + R125	1.030	[111]	R134a + R1234ze(E)	1.000	[96]			
R161 + R227ea	1.030	[112]	R125 + R1234yf	1.000	[110]			
R152a + R134a	1.000	[113]	R125 + R1234ze(E)	1.000	[114]			
R152a + R125	1.000	[115]	R245fa + R1234ze(E)	1.000	[116]			
R152a + R245fa	1.000	[117]	R227ea + R1234yf	1.000	[118]			
R152a + R227ea	1.000	[101]	R227ea + R1234ze(E)	1.000	[119]			
R134a + R125	0.993	[120]						
R134a + R245fa	1.000	[121]						
R134a + R236fa	1.000	[122]						
R134a + R227ea	0.990	[101]						
R125 + R245fa	0.985	[123]						
R125 + R236fa	0.980	[100]						
R125 + R227ea	0.990	[124]						

using *PH* and *TS* diagrams predicted from the molecular model at the chosen conditions with ideal gas enthalpy (H^{IG}) and entropy (S^{IG}) correlations from NIST REFPROP database for each refrigerant [52], with the iteration subroutines developed using polar soft-SAFT included in Fig. S2 in the SI.

The non-monetized key performance indicators (KPIs) for technical evaluation of drop-in replacement blends are based on volumetric cooling capacity (VCC), discharge line temperature (DLT), and condenser pressure (P_{cond}), which should be like the replaced refrigerant to ensure high system compatibility and minimal retrofitting. Other thermodynamic properties and performance criteria were included to assess the degree of blend compatibility including NBP, pressure ratio (P_R), suction density (ρ_v), refrigeration effect (RE), power per ton of refrigeration (PPTR) and coefficient of performance (COP), predicted in a similar manner as in previous work [14]. Promising blends are those minimizing NBP, P_R and PPTR, while maximizing RE, ρ_v and COP. Additionally, the exergetic efficiency (η_{II}) was also estimated to gain additional insight on the effectiveness of the designed blends [130–134], computed with the mathematical formulation in **Eqs. S1 and S2 in the SI**. The accuracy of computing these KPIs **depends on the accuracy of the thermodynamic model in predicting the required thermodynamic properties for their calculations, which are within 0.05 % for enthalpy, 0.86 % for entropy, and 2.11 % for density based on evaluation for predicted blend properties from polar soft-SAFT compared to those available from REFPROP** [52].

These technical criteria were used to determine the compatibility of the short-listed blends in *SS*-VCRC cycles operated with R134a and R410A, with potential blends having a KPI value equal to, less than, or larger than those predicted for R134a or R410A from polar soft-SAFT, depending on the KPI. For the sake of simplicity, these technical KPIs were lumped in a single value based on equal weights given for each metric included in Table 4, with promising blends selected based on a 90 % compatibility ratio, for further evaluation in terms of overall environmental impact, and projected yearly system cost.

2.4. Environmental evaluation of promising drop-in replacement blends

The environmental impact associated with their utilization and emissions to replace R134a and R410A was evaluated employing the total equivalent warming impact (TEWI) metric [135]. TEWI is a measure of the global warming impact derived from the direct (*i.e.,* refrigerant leakage and end-of-life disposal) and indirect (*i.e.,* compressor energy consumption) GHGs emissions related to the utilization of the refrigerant in the intended application, in terms of yearly tons of equivalent CO_2 emissions, as:

$$TEWI = \{GWP\cdot((L\cdot m\cdot n) + (m\cdot(1-\alpha)))\}_{Direct} + \{E_a\cdot\beta\cdot n\}_{Indirect} \quad (4.a)$$

$$E_a = \omega_{comp}\cdot\dot{m}\cdot AOT = \omega_{comp}\cdot\left(\frac{\dot{Q}_{ev}}{RE}\right)\cdot AOT = \left(\frac{\dot{Q}_{ev}}{COP}\right)\cdot AOT \quad (4.b)$$

where, L is the annual leakage rate, m is the refrigerant charge load, n is the system operating life, α is the recovery or recycling factor, E_a is the system yearly energy consumption, β is the country-dependent indirect emission factor, $\omega_{compressor}$ is the net cycle compressor's work, $\dot{m}_{ref}$ is the refrigerant mass flow rate, $\dot{Q}_{ev}$ is the cooling capacity, RE is the refrigeration effect, and AOT is the annual operation time. The values for these parameters are provided in Table S3 in the SI. Notice that, with this metric, the environmental assessment of these blends not only accounts for their GWP, but also includes the indirect impact associated with the energy consumption of the VCRC cycle (E_a). This is dependent on the type and efficiency of the cooling system, the properties of the refrigerant blend, and the level of decarbonization in the energy mix (*i.e.,* fuel type) within a specific country by considering the country-dependent indirect emission factor (β).

2.5. Economic analysis of promising drop-in replacement blends

The total annualized cost (TAC, $\dot{C}$) for deploying the promising refrigerants blends in the VCRC cycle includes the capital (CAPEX, $\sum\dot{C}_k$), operating and maintenance (OPEX, $\dot{C}_{op}$), environmental (Enviro, $\dot{C}_{env}$), and set-up (C_{set-up}) costs, utilized as monetized KPIs for determining the optimal drop-in refrigerant blend, calculated according to **Eq. 5** as:

$$\text{TAC}\ \left(\$\cdot y^{-1}\right)\dot{C} = \sum\dot{C}_k + \dot{C}_{op} + \dot{C}_{env} + C_{set-up} \quad (5.a)$$

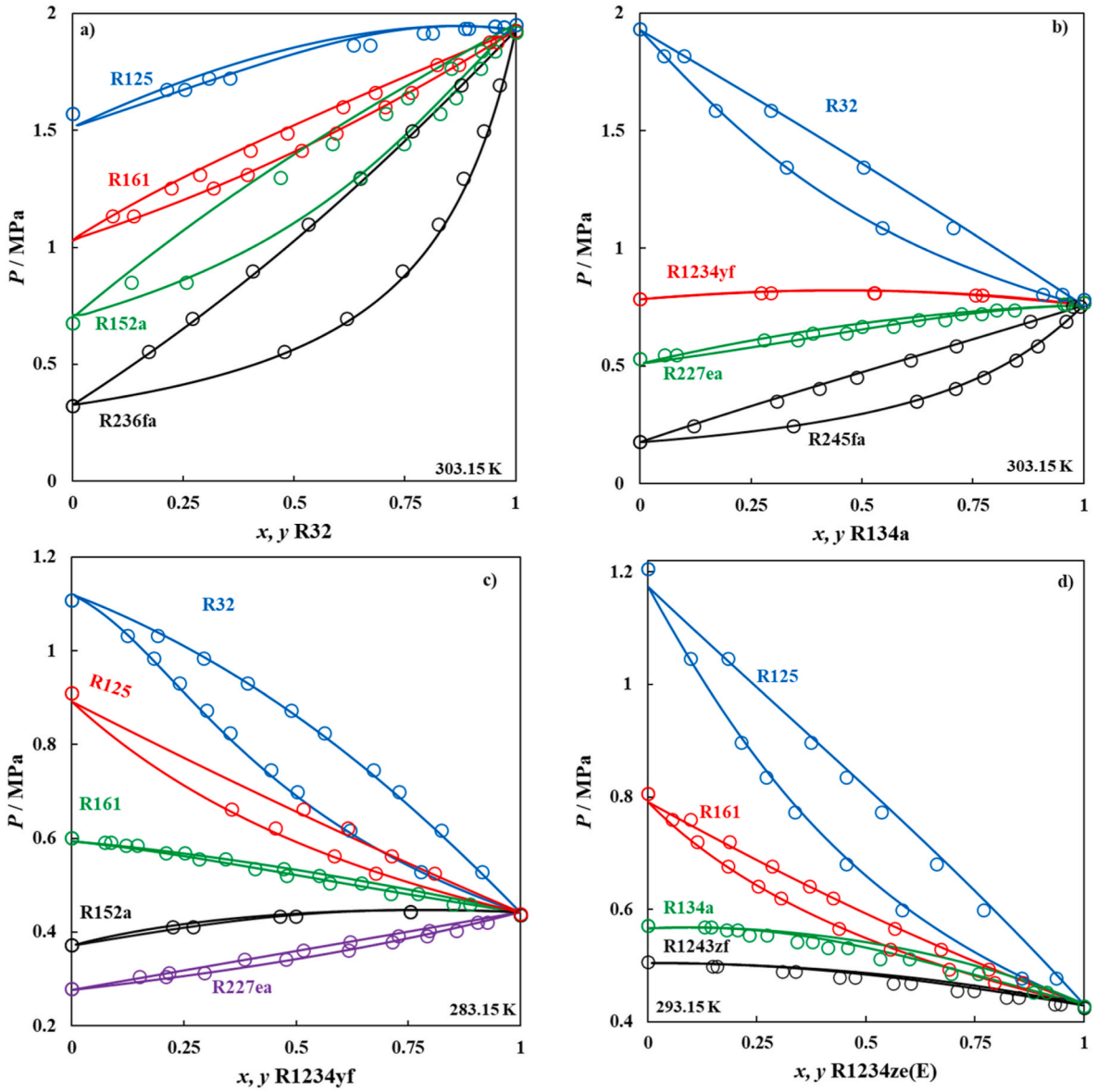

Fig. 1. VLE of selected refrigerants binary mixtures for those containing **a)** R32, **b)** R134a, **c)** R1234yf and **d)** R1234ze(E), using polar soft-SAFT (solid lines), compared to experimental data (symbols) from other studies (see Table 3).

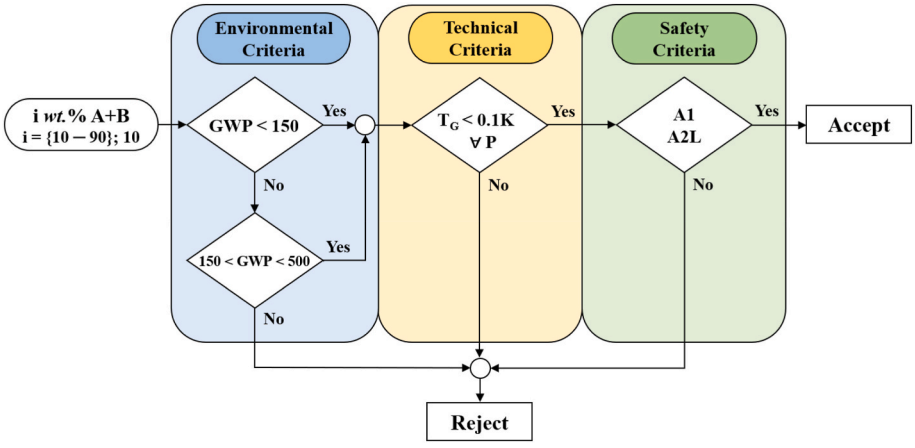

Fig. 2. Initial screening criteria for blend selection based on environmental, technical, and safety criteria.

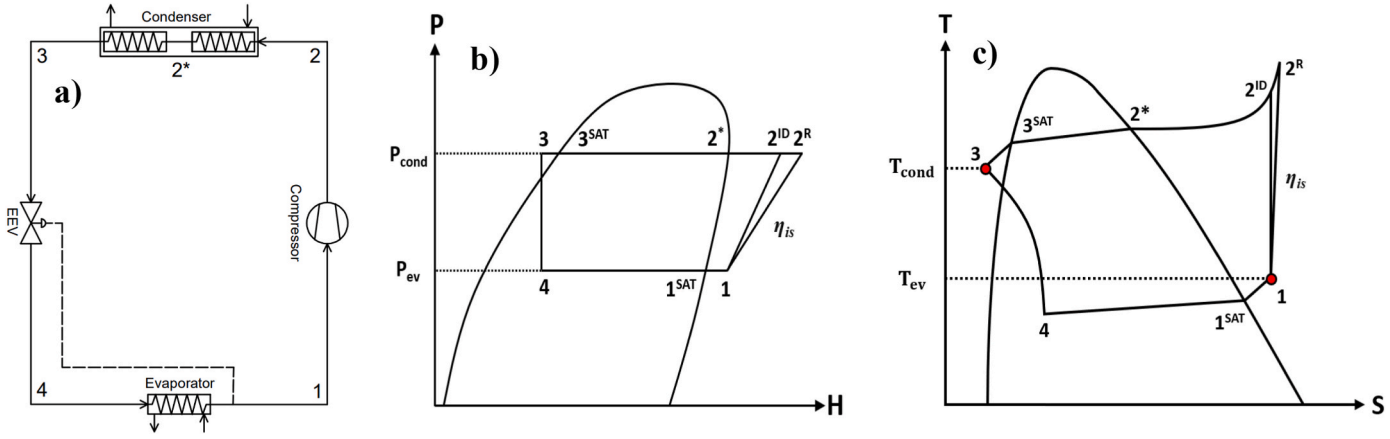

Fig. 3. A) Schematics for the basic *SS*-VCRC refrigeration cycle simulated in this work with its corresponding **b)** *PH* and **c)** *TS* diagrams.

Table 4
KPIs for technical evaluation of drop-in replacement refrigerant blends for R134a and R410A.

Criteria	Definition	Variation to HFCs
Drop-in KPIs		
Volumetric Cooling Capacity (*VCC*)	$VCC = (H_1 - H_3)\cdot\rho_V$	Equalized (=)
Discharge Line Temperature (*DLT*)	$DLT = T_{2^R}$	
Condenser Pressure (P_{cond})	$P_{cond} = P_2 = P_{2^*} = P_3$	
Other thermodynamic properties and performance metrics		
Normal Boiling Point (*NBP*)	$NBP = T_{atm}^{SAT}$	Minimized (−)
Pressure Ratio (P_R)	$P_R = P_{cond}\cdot P_{ev}^{-1}$	
Power Per Ton of Refrigeration (*PPTR*)	$PPTR = 3.5167\cdot COP^{-1}$	
Suction Density (ρ_V)	$\rho_V = \rho_1$	Maximized (+)
Refrigeration Effect (*RE*)	$RE = H_1 - H_3$	
Coefficient of Performance (*COP*)	$COP = \frac{H_1 - H_3}{H_{2^R} - H_1}$	
Exergetic Efficiency (η_{II})	$\eta_{II} = 1 - \left(\frac{\sum \dot{\chi}_d}{\sum \dot{\chi}_{in}}\right)$	

$$\text{CAPEX } (\$\cdot y-1)\sum \dot{C}_k = \frac{C_k \times \varphi}{3600 \times AOT}\cdot CRF = \frac{C_k \times \varphi}{3600 \times AOT} \times \left(\frac{i(1+i)^n}{(1+i)^n - 1}\right) \quad (5.b)$$

$$\text{OPEX } (\$\cdot y-1)\dot{C}_{op} = \sum \dot{W} \times AOT \times \alpha_{el} \quad (5.c)$$

$$\text{Enviro } (\$\cdot y-1)\dot{C}_{env} = m_{CO_2,e} \times c_{CO_2} = (\beta \times E_a) \times c_{CO_2} \quad (5.d)$$

$$\text{Set}-\text{up } (\$)C_{set-up} = m' \times (RP + Tax_{HFC}) + Tax_{CO_2}(GWP \times [m \times L \times n + m(1-\alpha)]) \quad (5.e)$$

$$\text{Lifetime load } (kg)m' = m + m \times L \times n \quad (5.f)$$

In estimating the capital cost of the *SS*-VCRC cycle with the different promising blends, the main equipment shown in Fig. 3 were considered, employing the unit cost functions provided in Table S4 in the SI [136–138]. Notice that the expression for the CAPEX accounts for the installation cost of each equipment in the cycle with a capital recovery factor with a 14 % annual interest rate (*i*) over the life time of the system (*n*) of 15 years with an annual operating time (*AOT*) of 8760 h, in addition to an allowance for system maintenance with a maintenance factor (φ) of 1.06 [137–140]. The operating cost accounts for the electricity consumption required for running work-consuming devices such as compressors in terms of compressor work ($\dot{W}$), with an additional allowance for the variation in electricity unit cost (α_{el}) [137,139,140], for different regions.

An additional monetized metric was included to account for the CO_2 penalty cost rate based on the annual GHGs emissions ($m_{CO_2,e}$) resulting from the energy consumption required for the VCRC cycle startup and operation, dependent on parameters affecting the indirect emissions in the TEWI assessment (*i.e.*, E_a and β) [137,139]. Additionally, the environmental cost accounts for the country-dependent average costs of CO_2 emissions avoidance (c_{CO_2}) from the integration of natural gas combined cycle power plants with carbon capture plants.

The last considered monetized metric was the set-up cost of the cooling unit inclusive of the cost of initial refrigerant load charged in the startup of the cooling cycle (*RP*), cost for additional 12.5 % per annum recharge load accounting for refrigerant leakage rate over the unit's lifecycle, taxes on utilization of HFC-based refrigerants based on the most restrictive legislation found under the Spanish restrictive tax law on F-gases [141], and taxes on direct CO_2-equivalent emissions associated with the refrigerant annual leakage over the system's life cycle and the end-of-life disposal of the remaining refrigerant load. The HFC utilization tax is a measure to reduce the import of bulk HFCs, while incentivizing the development and consumption of next-generation refrigerants. Comparable levies are applied in Denmark since 2001, leading to a significant decline in the import of bulk HFCs whilst moving towards a low carbon-based economy. The CO_2-eq tax might seem analogous to HFC utilization tax, however, the latter merely accounts for the tariff imposed on importing high-GWP cooling agents, while the former accounts for the associated negative environmental impacts from their emissions *via* leakage or end-of-life disposal (partial recycling), a factor typically overlooked in economic analysis of next generation refrigerants. This is added as a monetized KPI to allow examining the role of governmental policies on the development of consistent regulation to discourage the utilization of HFCs primarily focused on their environmental impact. The values for the parameters estimating the TAC of VCRC systems employing promising designed blends are provided in Table S3 in the SI.

3. Results and discussions

3.1. Short-listed refrigerant blends based on initial screening criteria

The initial screening of the 432 combinations of blends encompassing the 48 mixtures with different proportions was based on three conditions: (1) non-toxic low-GWP blends, either GWP <150 (study A), or 150 < GWP <500 (study B), (2) $T_G \leq 0.1$ K at a pressure range of (0.1–3 MPa), and (3) A1 or A2L flammability class. 12 candidates were identified, with 8 blends for study A, and 4 for study B, included in Table 5.

The environmental constraints on GWP accounted for the largest

Table 5
Short-listed refrigerant blends and their compositions based on initial screening criteria.

ID	Blend	*wt.*%[±]	GWP	T_G (K)[a]	ASHRAE class
Study A					
1	R1123 + R32	90.0	70	0.099	A1
2	R1234yf + R134a	90.0	130	0.010	A1
3	R1234yf + R152a	90.0	14	0.004	A2L
4		80.0	28	0.067	
5	R1243zf + R1234ze(E)	60.0	<1	0.041	A2L
6		70.0		0.012	
7		80.0		0.002	
8		90.0		0.000	
Study B					
1′	R1234yf + R134a	70.0	390	0.019	A1
2′		80.0	260	0.000	
3′	R1234ze(E) + R227ea	90.0	336	0.013	A1
4′	R152a + R134a	80.0	370	0.084	A2L

[±]The mass fraction for the 1st component in the blend.
[a] Obtained at atmospheric pressure (0.1 MPa).

exclusion rate (≈62 %). Note that the acceptable combinations under EU guidelines [4] on GWP <150 include HFCs + HFOs, and HFOs + HFOs blends, with the latter type achieving diminished pollutants capacities (GWP <1). Conversely, transitionary limits on GWP, study B, allowed for the inclusion of HFCs + HFCs blends as those commercially available. However, blends with R245fa were excluded on account of its toxicity. The limits on GWP in study A are in line with those implemented in developed countries including USA, UK, and EU states, with the stringent guidelines on allowable GWP limits playing a major role by including HFOs in the pool of promising replacement refrigerants, the lowest GWP seen for blends 5–8 (from Table 5), fully composed of HFOs. Although blends 1–4 possess GWP below required EU limits, their adoption in developed countries might be limited considering tariffs on HFCs utilization and import [22]. This will impact the imports of HFCs from major producers such as China and India. Conversely, the more relaxed limits in study B in developing countries such as China and India, might ensure the sustenance of HFCs manufacturers and their resistance to switch to HFOs production and manufacturing, considering that the HFCs market still endures with the production of pure HFCs, or HFCs-based blends. However, blends 1′– 4′ have nearly 50 % lower GWP compared to the commercial R134a in circulation. These blends, if compatible as drop-in replacements, might present a compromise solution that permits HFC manufacturers to continue with their business-*as*-usual agendas, while circulating low GWP refrigerants.

In terms of degree of azeotropy, the formulation of near-azeotropic blends was more flexible than fully azeotropic blends, with only two blends recognized as fully-azeotropic ($T_G = 0.000$ K). Predictions from polar soft-SAFT established that dipolar refrigerants with relatively similar normal boiling points (ΔNBP <5 K) and high structural similarity can easily result in near-azeotropic blends [142]. This can be seen in Fig. 4 from the reduced T_G magnitude for blends with R134a compared to R152a, denoting increased azeotropy for R1243yf + R134a due to similar molecular structures and polarity. The T_G predictions for the remaining blends in Table 5 are provided in Fig. S3 in the SI.

The flammability assessment for blends satisfying GWP and T_G limits is provided in Fig. 5. Plotting T_{ad} *vs.* $\frac{F}{F+H}$ conveniently allowed grouping the pure refrigerants and blends into different flammability regions corresponding to the ASHRAE classifications (A1, A2L, A2, and A3) [15]. The validity of the empirical approach is assured from the consistent flammability rating of known pure refrigerants and commercial blends with ASHRAE Standards [143–146], with A1 class for R134a and commercial blends (*i.e.,* R410A, R513A and R450A), and A2L classification for R32, R1234yf and R1234ze(E).

Based on Fig. 5, non-flammable A1 blends with $\overline{\Pi} \leq 0$ include those composed of R1234yf + R134a at different compositions (blends 2, 1′, and 2′), in-line with research findings [143]. The increase in $\overline{\Pi}$ for these blends is from the increased proportion for the A2L R1234yf. Another non-flammable blend is R1234ze(E) + R227ea (blend 3′), with similar

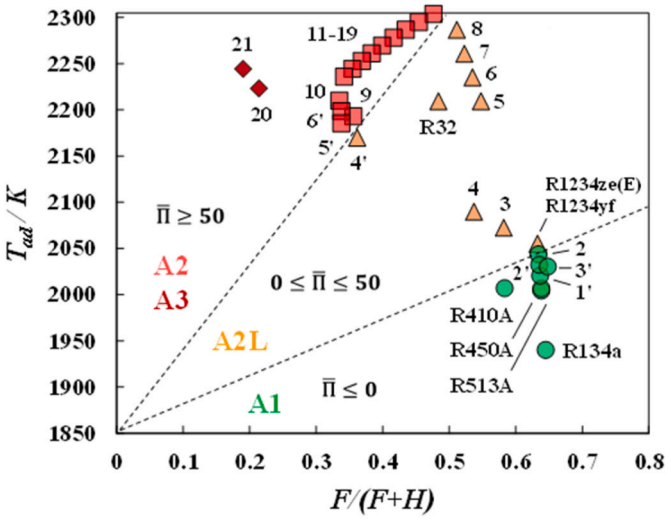

Fig. 5. Flammability assessment using T_{ad} and $F/(F + H)$ for pure refrigerants and blends. The dashed lines represent the regions of different flammability. Colors and symbols correspond to the flammability of the refrigerants and blends: green circles for A1, yellow triangles for A2L, red squares for A2, and dark red diamonds for A3, while the numbers correspond to the blends presented in Table 5 and Table S5 in the SI.

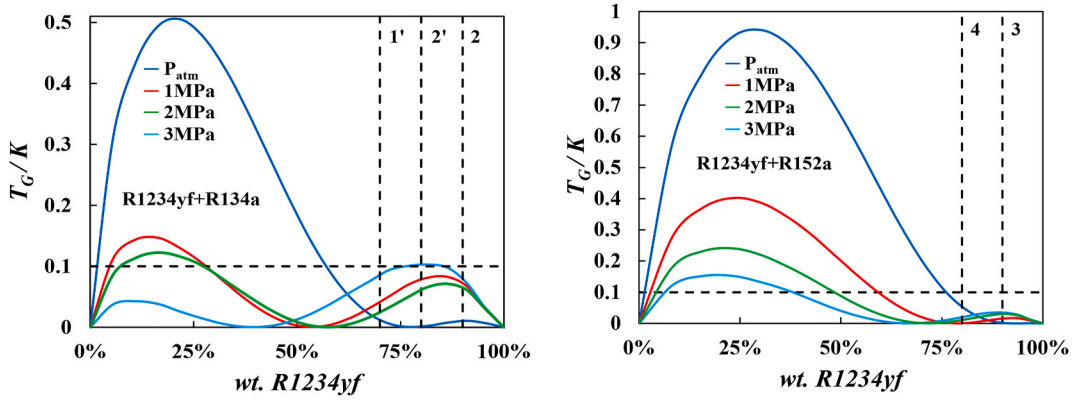

Fig. 4. Glide temperature versus weight percentage of the first component of the binary blend, at different pressures, for R1234yf + R134a blend (**left**), and R1234yf + R152a (**right**) as predicted from polar soft-SAFT. Dashed vertical lines denote blends from Table 4.

formulation to the commercial A1 blends R515A (88 *wt*% R1234ze(E)) and R515B (91 *wt*% R1234ze(E)) [144,145]. Other potential blends are those in the mild-flammability region (A2L), including blends 3 and 4 with R1234yf + R152a, similar to R32. However, these blends are positioned in the lower mild-flammability area, promising lower rates of increasing pressures in the case of explosion than R32 [146]. Additionally, blends composed of R1243zf + R1234ze(E) (blends 5–8) are within the mild-flammability region, with increasing degree of flammability with higher content of the A2 R1243zf. Interestingly, the presence of 10 *wt*% of the A2L R1234ze(E) was sufficient to reduce the flammability of blend 8. Several low-GWP blends with the required T_G (see Table S5 in the SI) were rejected due to their flammability including R152a + R1234ze(E) (blends 9 and 10), R152a + R1243zf (blends 11–19), and R152a with R227ea or R134a (blends 5′ and 6'), due to the high content of A2 R152a, and R1243zf.

The flammability of R32 + R1123 (blend 1) cannot be assessed with this method due to the lack of R1123 adiabatic flame temperature data. However, a recent study [16] clarified that similar blends with more than 60 mol% R1123 can be safely operated at typical operating conditions. As such, blend 1 can be expected to be A1 class owing to its 10 *wt* % R32 content.

3.2. Drop-in assessment and technical compatibility of low-GWP blends in SS-VCRC

The short-listed blends in Table 5 were evaluated as drop-in replacements for R134a and R410A. Additionally, the single-component refrigerants (*i.e.,* R32, R1234yf, R1234ze(E), and R1225ye(Z)) [14], and commercial blends R450A, and R513A were included for comparative purposes. The drop-in KPIs in Table 4 include equivalent VCC, DLT, and P_{cond}, to ensure minimal system retrofitting.

For the drop-in assessment for replacing R134a, several low-GWP designed blends, mostly HFCs + HFOs, proved to be highly compatible with similar VCC and P_{cond} values to R134a albeit lower DLT values as shown in Fig. 6. These include blends of R1234yf with 10–20 *wt*% of either R134a or R152a (blends 2–4). The compatibility of these blends was slightly better than the proposed alternative R513A for most drop-in KPIs, indicative of minimal compressor retrofitting. This can be attributed to the increased presence of R1234yf, which as a pure working fluid demonstrated a high potential for replacing R134a in some applications [14]. Although pure R1234yf was slightly better than its blends in terms of VCC and P_{cond}, the presence of other refrigerants in these mixtures helped increase the DLT. The advantage offered by these blends also includes their low-GWP (14–130) compared to the higher GWP of R513A (GWP = 608), facilitating the full transition to low-GWP refrigerants.

Concurrently, increasing the content of R134a (20–30 *wt*%) in its blend with R1234yf (*e.g.,* blends 1′ and 2') was also technically compatible for replacing pure R134a, with a lower GWP in-line with interim transition stages (*i.e.,* study B with 150 < GWP <500). The compatibility of these blends was within 5 % increased VCC and P_{cond}, however, with lower DLT values, also resulting in minimal system retrofitting. Notice the improved lower flammability rating of HFC + R1234yf blends, moving from A2L (blends 3 and 4) to A1 (blends 2, 1′ and 2') with increasing proportions of the A1 R134a as opposed to the A2 R152a. Moreover, the only HFO + HFO blend with negligible GWP offering an acceptable compromise among the three KPIs was 60 *wt* % R1243zf + R1234ze(E) (blend 5), however, with an A2L flammability similar to R32 (see Fig. 5).

Finding a replacement for R410A was a more challenging task as shown in Fig. 6. The single-component R32 was the most compatible drop-in replacement with its similar VCC and P_{cond}, however, with larger DLT, which would present an environmental advantage to R410A, but remains infeasible considering the upcoming GWP requirements. Among the designed blends, 90 *wt*% R1123 + R32 (blend 1) had the only acceptable KPI magnitudes as R410A replacement, due to the presence

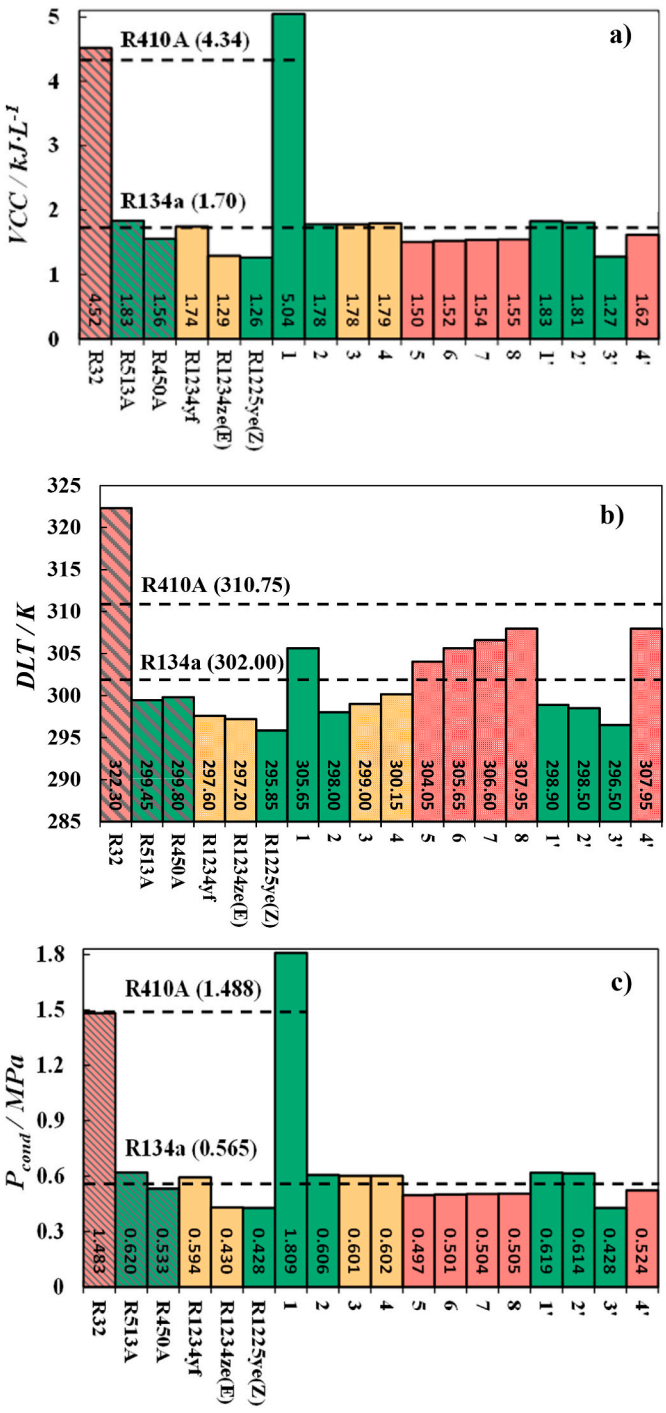

Fig. 6. Drop-in assessments for blends in Table 5 based on KPIs, **a)** VCC, **b)** DLT, and **c)** P_{cond}, for replacing commercial R134a and R410A. Note the bar color corresponds to the flammability class, with A1 (green), low A2L (yellow), and high A2L (red). The bars with denote refrigerants and blends with GWP >500. The numbers on the lines and in the bars correspond to the values of each KPI.

of R32, yet being capable of meeting environmental and safety targets (GWP = 70 and A1 rating). Note the complete absence of suitable alternatives for the transitionary stage. System retrofitting would be inevitable when replacing R410A with low-GWP alternatives. In recent studies, operational challenges for R32 as a replacement for R410A were highlighted such as hazardous compressor DLT and shortened compressor lifetime, require several retrofits to enhance the system lifetime [147,148]. Therefore, it is reasonable to carry out such

modifications with blend 1, or any other suitable candidates.

Additional thermophysical and technical performance properties (*i.e.,* NBP, P_R, ρ_V, RE, PPTR, η_{II}, and COP) for the most promising blends based on the drop-in KPIs are shown in Fig. 7, for a comparative analysis based on the criteria rating provided in Table S6 in the SI. A closer examination of these properties revealed relative similarities with R134a for all promising blends (*i.e.,* blends 2–5, 1′ and 2') with acceptable changes within 5 % for NBP, P_R, PPTR, and COP. Larger changes were observed for ρ_V, and RE, indicative of lower system efficiency, and increased refrigerant mass flow rate directly affecting operational costs [149]. A similar outcome was seen for blend 1 for replacing R410A, with slightly better thermophysical properties than R32, however, significantly lower RE, PPTR, η_{II}, and COP values.

The most compatible blends (>90 %) for replacing R134a, in Table 6, include blends 2–5, and blends 1′ and 2', with the highest compatibility for blend 3, outperforming commercial blends R513A and R450A, and single-component refrigerants. In contrast, the only feasible blend for replacing R410A was blend 1, achieving a similar compatibility ratio (73 %) to R32. These results were consistent irrespective of the operating conditions in Fig. S4 in the SI.

3.3. Environmental impact of promising low-GWP blends

The previous results established the viability of blends 1–5, 1′ and 2′ designed in this work as drop-in replacement blends for R134a and R410A. This section focuses on the overall environmental impact of these blends associated with their utilization and emissions in refrigeration cycles quantified in terms of the TEWI metric. The analysis considered major global HFCs producers including the People's Republic of China (PRC), United States of America (USA), European Union (EU), Japan, and India [150], some of which have significantly contributed to current legislations on HFCs emissions and consumption (*i.e.,* USA, EU and Japan) [151]. The parameters required for the TEWI evaluation are included in Table S3 in the SI, with the technical cycle performance evaluated from polar soft-SAFT, and results are presented in Fig. 8.

The level of direct emissions related to the leakage rate and end-of-life cycle disposal of the refrigerants were similar across all examined geographical areas (see Fig. 8, top), as the parameters concerning their estimations were fixed beforehand. This is simplistic for the sake of convenience; however, it suffices for a comparative analysis. Conversely, indirect emissions related to the energy consumption for system operation using the examined refrigerants varied across the different regions, attributed to the carbon footprint of the different energy resources, with the largest impact seen for India (dependent on fossil fuels), while the lowest was for EU (mostly dependent on renewable energy resources). Additional evaluation for the top-12 most densely populated EU states, with more than 85 % of the EU's overall population (see Fig. 8, bottom), demonstrated the high level of direct emissions in Poland (POL) compared to the lowest levels in Sweden (SWE) and France (FRA), as the former largely depends on fossil fuels for energy consumption, while the latter two are more oriented towards renewable, particularly hydro and offshore wind power, and nuclear energy consumption, respectively. The dissimilar contributions of direct and indirect emissions demonstrate the relevant role of the degree of decarbonization of the energy mix, the effect of the refrigerant on cycle

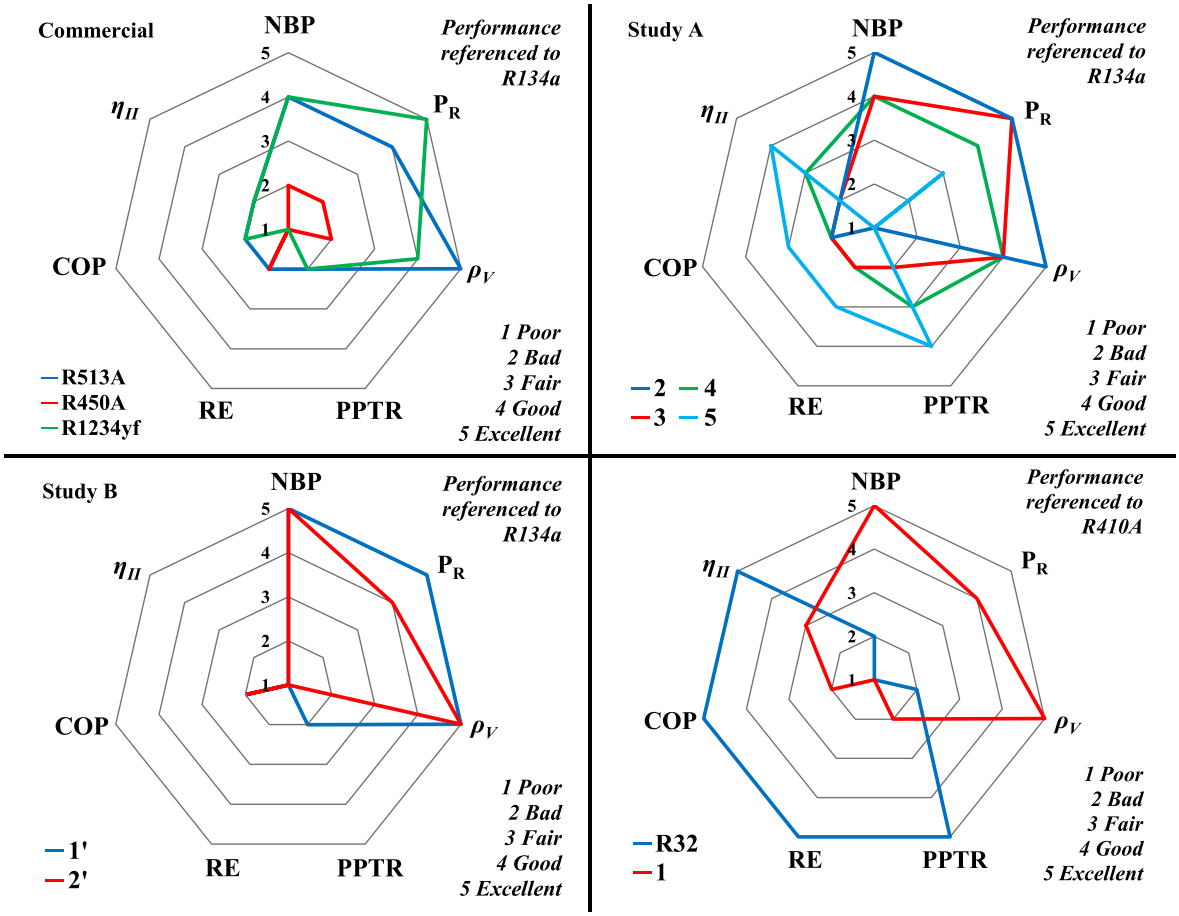

Fig. 7. Comparative analysis for thermophysical properties and technical performance criteria of promising drop-in blends compared to R134a and R410A. **Top left:** available commercial refrigerants performance referred to R134a; **top right:** selected refrigerants included in study A referred to R134a; **bottom left**: selected refrigerants included in study B compared to R134a; **bottom right**: refrigerant 1 and R32 performance referred to R410A.

Table 6
Compatibility analysis of promising blends designed in this work for replacing R134a and R410A. Compatibility codes designate null (≥90 % - green), partial (yellow), and complete (≤60 % - red) – retrofitting required.

		R32	R513A	R450A	R1234yf	R1234ze(E)	R1225ye(Z)	1	2	3	4	5	6	7	8	1'	2'	3'	4'
Performance 1: Poor 2: Bad 3: Fair 4: Good 5: Excellent	Π	3	5	5	4	4	5	5	5	4	4	3	3	2	2	5	5	5	3
	NBP	4	2	2	2	5	1	5	2	2	2	1	2	2	2	2	2	1	2
	P_R	4	3	2	3	2	1	5	3	3	3	2	2	2	2	3	3	2	2
	ρ_V	5	3	2	3	2	1	5	3	3	3	2	2	2	2	3	3	1	2
	RE	4	1	1	1	1	1	1	1	1	1	2	2	2	2	1	1	1	3
	PPTR	3	3	2	3	4	3	1	3	3	4	5	5	5	5	3	3	4	5
	COP	3	3	2	3	4	3	1	3	3	4	4	4	4	5	3	3	4	5
	η_Π	3	3	1	3	4	3	1	3	3	4	4	4	5	5	2	3	4	5
Drop-in KPIs R134a	VCC	1	4	4	5	2	2	1	5	5	4	4	4	4	4	4	4	2	4
	P_{cond}	1	5	5	5	4	4	1	5	5	5	5	5	5	5	5	5	4	5
	DLT	1	5	5	4	3	2	4	4	5	5	5	4	3	3	5	5	3	4
Drop-in KPIs R410A	VCC	5	1	1	1	1	1	4	1	1	1	1	1	1	1	1	1	1	1
	P_{cond}	5	3	2	3	2	2	4	3	3	3	2	2	2	2	3	3	2	2
	DLT	1	1	1	1	1	1	3	1	1	1	2	3	4	5	1	1	1	5
Compatibility / %	R134a	20	93	93	93	60	53	40	93	100	93	93	87	80	80	93	93	60	87
	R410A	73	33	27	33	27	27	73	33	33	33	33	40	47	53	33	33	27	53

energy consumption and its efficiency in reducing the environmental footprint for deploying low GWP refrigerants. Surely, a higher benefit can be obtained through combining low GWP refrigerants with renewable energy resources and high system efficiency to reduce both direct and indirect emissions levels. Both commercial refrigerants R134a and R410A presented the highest direct emissions of 7.07 and 10.46 tCO_2-eq, respectively, closely related to their high GWP. Additionally, lower direct emissions were obtained with proposed commercial replacements R32 (1.77 tCO_2-eq), R450A (2.97 tCO_2-eq), and R513A (3.11 tCO_2-eq) within 50 % lower than 3rd generation refrigerants. Clearly, the synthetic blends from this work present a major reduction in direct emissions, being almost 90 % lower than R134a and R410A, with nearly negligible direct contributions for blends 1, 3, 4, and 5 due to the large proportion of low-GWP HFOs in these blends (*i.e.,* R1123, R1243yf, and R1243zf).

Overall, the environmental burden for blends 2–5 are the lowest with 8.9–11.4 % reduced environmental footprint from R134a. These are attractive alternatives, given also their high technical compatibility (>90 %) with R134a-operated systems indicative of lower retrofitting costs.

Regardless of the producing country, the market availability and current relative prices for these refrigerants are additional decision criteria to be included. For instance, the estimated price for blends 2' and 2–4 can be approximately 5 times that of R134a ($12.9 per kg), based on the retail price of the individual constituents [152,153]. The cheapest R134a drop-in replacement corresponds to blend 5 with a relative cost of $45 per kg. Though HFC prices are lower, their economic attractiveness drops due to imposed utilization taxes [4], with an additional cost of $21.5–31.3 per kg for R134a or R410A [141]. Surely, the economics of scale will eventually play its role in reducing the prices of alternative refrigerants once their adoption becomes more widespread.

3.4. Economic evaluation for deploying promising low-GWP blends

The last evaluation is focused on the economic assessment of designed blends using monetized KPIs associated with capital, operating, environmental, and setup. Provided in Fig. 9 is the total annual cost for deploying the designed blends and their benchmark commercial alternatives including cost variability in terms of country of deployment, computed on the basis of the *SS*-VCRC cycle for the major producers of R134a (Fig. 9a) and R410A (Fig. 9b). Similar assessment for each member of the EU is provided in Fig. S5 in the SI.

The capital and maintenance costs had the largest contributions to TAC, consistent within the different countries, as they are dependent on the cost of manufacturing the operating units. The OPEX associated with the energy consumption for the operation of the cooling cycles are the second largest, affected largely by geographical location and its associated cost of electricity, and to a smaller degree by the type of refrigerant and its impact on the cycle's efficiency. Higher operating costs are associated with EU and Japan, due to the higher cost of electricity, as opposed to lower OPEX in India due to the consumption of coal. The variation in OPEX due to refrigerants are less effective compared to cost of electricity, with the variation attributed to the impact of the refrigerant on the energy consumption, with similar OPEX levels to R134a seen with blend 5 due to similar COP, and slightly higher OPEX for blend 1 replacing R410A due to lower COP than R410A.

Conversely, the lowest contributions are seen for the environmental and setup costs associated with the taxes on the CO_2 emissions from power consumption, the environmental impact of the refrigerant and its retail price, accounting for approximately 5.7 % of the total costs. These cost factors are more indicative of the role of governmental and regulatory agencies on instilling barriers on adoption and deployment of technologies with high carbon footprint. Among major HFC producers, the largest environmental costs are seen in India, owing to the environmental burdens from the utilization of the high-carbon emitting coal

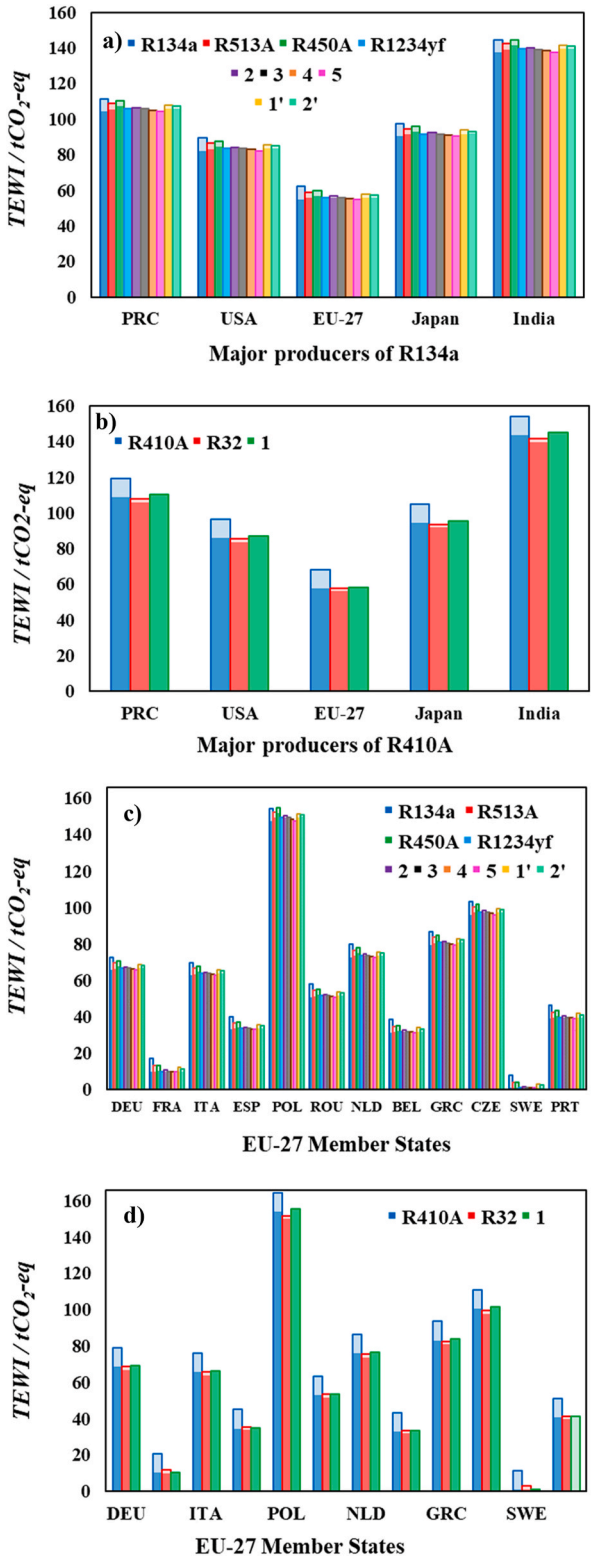

Fig. 8. TEWI analysis for most promising alternatives for R134a (**a and c**) and R410A (**b and d**), with the bar colors corresponding to the studied benchmark refrigerants and designed blends, as per the legend inside the figures. **a) and b):** the different major HFCs producers, sorted by emission rates, and **c) and d):** selected EU countries, sorted by population from left to right. The strong color represents indirect emissions, while the light-equivalent color stands for direct emissions.

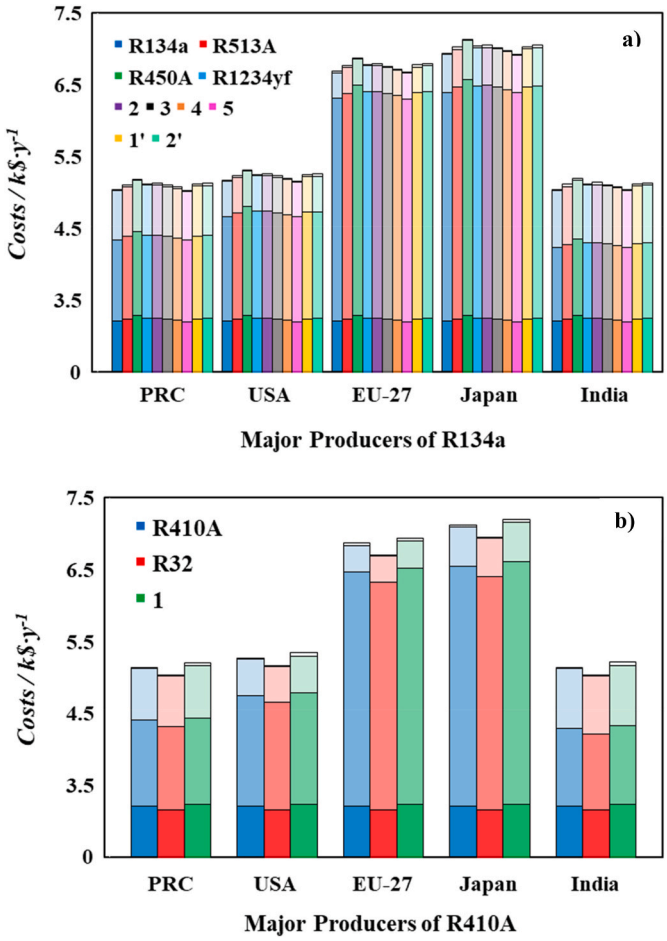

Fig. 9. Economic analysis for most promising alternatives for **a)** R134a and **b)** R410A, for the different major HFCs producers based on total annual costs. The colors represent the different refrigerants and blends, as per the legend inside the figures. The different portions of the bars represent the split of the total annual cost, from bottom to top (darker to lighter colors): CAPEX, OPEX, Enviro, and set-up costs, calculated from Eq. 5, utilized as monetized KPIs for determining the optimal drop-in refrigerant blend.

as a primary energy resource, though cheaper.

The economic viability of promising blends is in Fig. 10 as a country-dependent heatmap of additional TAC incurred from replacing current systems with R134a and R410A. Although blend 3 is highly compatible with R134a, the economic assessment showed additional retrofitting costs of 57.7–105.3 $\$\cdot y^{-1}$. Conversely, blend 5 is a better alternative than blend 3, resulting in cost savings (-18.3 $\$\cdot y^{-1}$) or marginal additional retrofitting costs, being more economically viable with relatively similar technical performance. Notice, that blend 5 is also more favorable based on environmental impact, with GWP <1 from its HFOs formulation, as opposed to blend 3 with GWP $= 14$, containing HFC. In a similar fashion, replacing R410A with the only feasible blend identified in this work, blend 1, would result in retrofitting costs in the range of 55.4–101.1 $\$\cdot y^{-1}$.

The economic viability of replacing R134a with blend 5, and R410A with blend 1 affected by geographical location with special emphasis on operating and environmental costs is provided in Fig. 11, as CAPEX remained country independent. A trade-off is observed between both monetized KPIs. The OPEX in India are among the lowest, however, the environmental cost is the highest. This is attributed to its reliance on the cheaper coal for power generation, however, with high CO_2 emission factor, also seen with Poland in the EU. This was not found in the USA, given its reliance on the relatively cleaner natural gas, resulting in 38.8 % reduced environmental costs on average. The picture is diverse for the

	5	4	1	3	1'	2'	2
DEU	-3.9	57.4	101.1	105.3	124.0	143.8	148.6
BEL	-3.7	52.0	92.6	93.9	111.7	129.7	135.2
DNK	-18.3	42.4	79.3	89.7	108.4	127.9	132.9
JPN	-3.7	50.3	89.9	90.3	107.9	125.3	131.0
ITA	-3.7	49.5	88.7	88.6	106.1	123.2	129.0
IRL	-18.2	40.1	75.6	84.8	103.0	121.8	127.0
AUT	-3.6	47.3	85.3	84.1	101.1	117.5	123.6
PRT	-3.6	47.1	85.0	83.7	100.8	117.1	123.2
CZE	-3.6	46.9	84.7	83.3	100.3	116.6	122.7
POL	-3.6	46.8	84.4	83.0	99.9	116.2	122.3
CYP	-18.2	37.0	70.7	78.3	96.0	113.8	119.4
GRC	-3.6	45.3	82.1	79.8	96.5	112.3	118.5
FRA	-3.5	44.7	81.2	78.6	95.3	110.8	117.1
ESP	-14.9	37.7	71.4	76.1	93.5	110.4	116.3
SWE	-3.5	43.9	80.0	77.0	93.5	108.8	115.2
EU-27	-10.4	39.3	73.5	74.8	91.7	107.7	113.9
ROU	-3.5	43.0	78.5	74.9	91.3	106.3	112.8
NLD	-3.5	41.7	76.4	72.2	88.4	102.9	109.6
EST	-18.1	33.7	65.6	71.5	88.7	105.4	111.3
USA	-3.4	39.8	73.5	68.3	84.1	98.0	104.9
BGR	-3.4	39.7	73.3	68.0	83.9	97.7	104.7
IND	-3.4	39.1	72.3	66.7	82.4	96.1	103.1
HUN	-3.4	38.0	70.7	64.5	80.0	93.4	100.5
PRC	-3.4	39.0	72.3	66.7	82.4	96.0	103.0
LVA	-18.0	30.5	60.5	64.6	81.2	96.8	103.1
LUX	-18.0	30.4	60.4	64.5	81.2	96.8	103.1
HRV	-3.4	39.1	72.3	66.7	82.4	96.1	103.1
FIN	-17.9	29.2	58.5	61.9	78.3	93.5	100.0
SVN	-17.9	29.1	58.4	61.7	78.2	93.3	99.8
SVK	-17.9	27.9	56.5	59.2	75.4	90.2	96.8
LTU	-17.9	27.5	55.8	58.3	74.4	89.0	95.7
MLT	-17.9	27.2	55.4	57.7	73.8	88.4	95.1
	Extra TAC vs HFC's / $\$\cdot y^{-1}$						

Fig. 10. Heat map for the variation in TAC (calculated from Eq. 5) of drop-in candidates benchmarked to R134a and R410A, respectively, ordered from highest to lowest. The main producers of HFCs are highlighted in light blue in the left column.

environmental costs in the USA due to varying electricity sources depending on the states, with cheaper environmental costs seen in Washington and Idaho states, and high costs similar to India seen in Wyoming state. Conversely, for the EU extremely low CO_2 emissions penalties are reported at the expense of elevated OPEX with the higher electricity prices, being a mixture of increased cost of imported energy resources for power generation and imposed environmental legislation on climate change. Within the EU, the lowest cost rates are found in Malta, Lithuania, and Slovakia with cheaper electricity prices, as opposed to Germany, Denmark, Belgium, and Ireland. Similar analysis for blends (2–4, and 1' – 2') is in Figs. S6 and S7 in the SI.

3.5. Sensitivity analysis on the role of policy to promote adoption of designed blends

A sensitivity analysis is presented here based on legislative agendas imposed on current HFC utilization that can be realistically implemented in upcoming years to boost the economic viability of next-generation refrigerants and effectively promote a transition to their manufacturing and market deployment. These involves examining the implementation of a tax-law analogues to CO_2 tax focused on direct HFC emissions through leakage and end-of life disposal, dubbed CO_2-eq tax, (Tax_{CO_2}), in addition to a multiplier on the current HFC utilization tax enacted in Spain to date (Tax_{HFC}), provided in Fig. 12, which has been applied on all studied systems with their baseline costs for EU provided in Fig. 10.

In this manner and taking the EU-ETS's pan-European carbon tax of $49.7\$\cdot tCO_2\text{-eq}^{-1}$ as a benchmark (see Table S3 in the SI), a significant variation in the cycle cost rate with change in the HFC tax multiplier was obtained, as depicted in Fig. 12. Blend 5 demonstrated baseline annual cost savings of $-10.4\ \$\cdot y^{-1}$ compared to R134a in EU, with increased savings with larger tax multiplier due to the absence of HFC from its composition. Additionally, considering that blends 1 and 4 had slightly higher annual costs compared R134a and R410A, respectively, it is observed that implementing a tax multiplier of 3.2 and 2.3, respectively would reduce the annual costs of blends 1 and 4 to those of their respective benchmarks, with higher tax multiplier promising annual cost savings compared to R134a and R410A.

If the Swedish carbon tax on direct emissions of $137.2\$\cdot tCO_2\text{-eq}^{-1}$ is enacted, blends 1, 4, or 5 would result in cost savings compared to R134a and R410A without the implementation of additional taxes on HFC utilization. Additionally, the use of blend 3 to be economically competitive to R134a would require a HFC utilization tax multiplier between 1.9 and 5.7 when the carbon tax on direct GHG emissions increases from \$49.7 tCO_2-eq (EU-ETS) to \$137.2 tCO_2-eq (SWE). Irrespective of the carbon tax limits, economic viability of blends 2, 1′, and 2' compared to R134a is achieve with HFC utilization tax multiplier >5.0 in Fig. S8 in the SI.

In summary, only blend 5 exhibits beneficial retrofitting costs when applying the EU-ETS carbon pricing proposal and the Spanish case law on HFC manufacturing. In essence, the high technical compatibility of blend 5 with current cycles operated with R134a, even with a potentially higher blend cost compared to R134a, alongside the impact of its thermodynamic properties on enhanced cycle efficiency and energy consumption are sufficient to ensure investment costs comparable to R134a. Notice that drop-in blends 4 and 1 are also covered by such selection criterion, yet with a 2.2 % increase HFC tax rate from those currently enacted by Spanish authorities. Accordingly, minor adjustments to current policies would be required to adjust the economics of scale to enhance the attractiveness of low GWP refrigerants.

4. Conclusions

A 4 E approach has been developed and implemented in this work for identifying low GWP refrigerants as drop-in replacements for R134a and R410A for cooling and refrigeration applications, based on technical KPIs, flammability, environmental and economic impact. The molecular-based polar soft-SAFT EoS was used as a reliable platform for generating missing properties needed for the rational design of binary blends composed of combinations of HFCs + HFCs, HFCs + HFOs, HFOs + HFOs, and HFOs + HCFOs. The validity of the thermodynamic model was proven from the excellent agreement with experimental data for the studied mixtures, allowing the reliable prediction of properties needed for further evaluation. The potential blends were narrowed down based on low-GWP, low temperature glide characterizing near-azeotropic

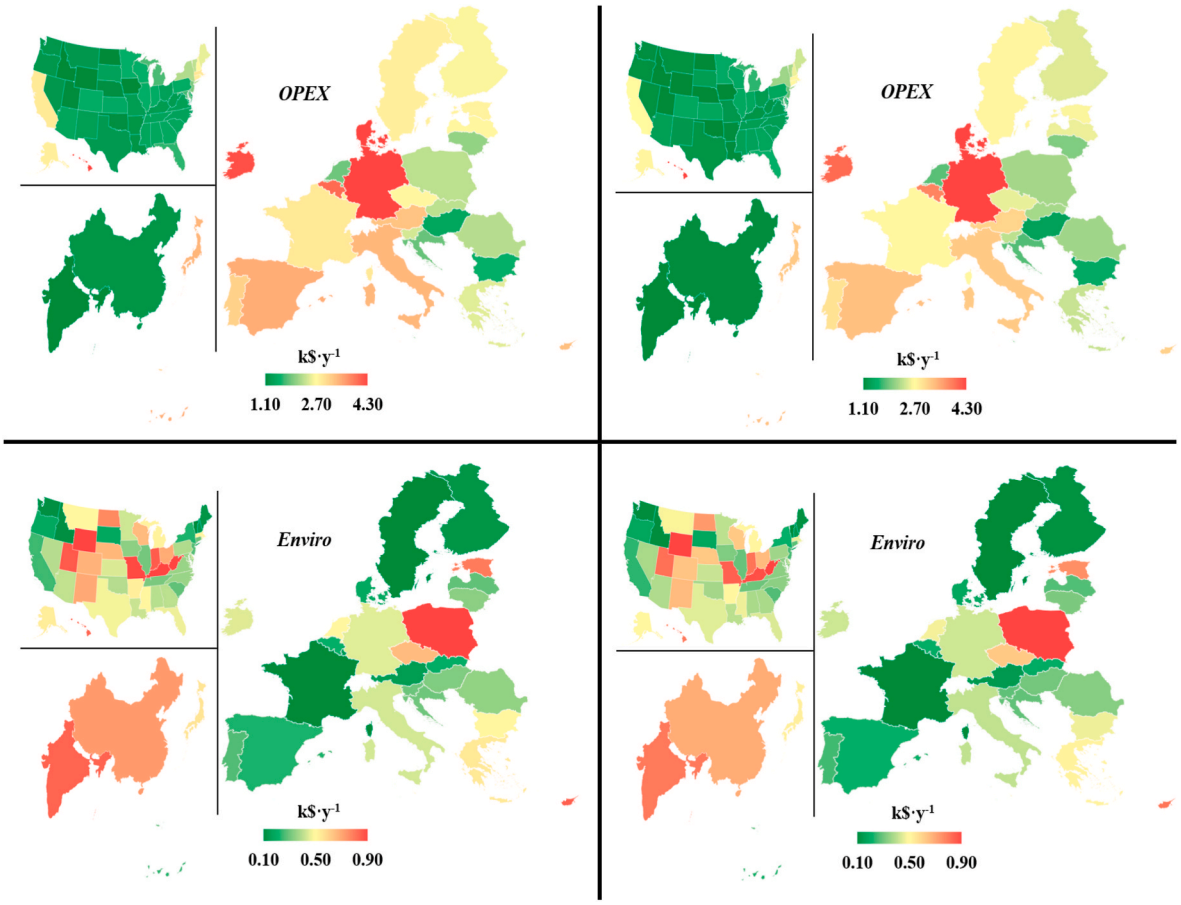

Fig. 11. Geographical variation in annualized operating (top) and environmental (bottom) costs for blend 1 (left), and blend 5 (right).

blends (≤0.1 K), and A1 or A2L safety classes.

Within the designed procedure, twelve potential blends were identified for further technical evaluation as drop-in replacements focused on KPIs, thermophysical properties, and technical performance criteria in *SS*-VCRC cycles. The most compatible designed blends for replacing R134a are those composed of R1234yf HFO with a small content (10 *wt* %) of HFCs such as R134a (blend 2) or R152a (blend 3), alongside HFO-based blend of (60/40) *wt.*% R1243zf + R1234ze(E), promising similar system performance with minimal modifications, although presenting mild-flammability versus the non-flammable R134a. Alternatively, limited options were found for replacing synthetic blend R410A, with the most acceptable trade-off established for pure R32 and its blend with R1123 (blend 1 of (90/10) *wt.*% R1123 + R32), highlighting the need for examining other refrigerant families to design suitable alternatives for R410A.

The deployment of the designed blends promises a 9–15 % reduction in environmental impact in terms of TEWI associated with direct refrigerant emissions *via* leakage and disposal, and indirect CO_2 emissions from energy required for operation. This is attributed to the low GWP of the designed blends, 100–1000 times lower than R134a and R410A.

Lastly, the total annualized costs for the deployment of the proposed replacements in existing systems operated with R134a and R410A were accounted for, considering country-related parameters for major HFC producers and consumers. Overall, larger country-related impacts were seen for OPEX and environmental costs, closely related to the energy mix and level of decarbonization, with developing countries such as India incurring lower OPEX on the expense of larger environmental costs, due to the consumption of high carbon fuels, while the opposite trends were seen with countries adoption low-carbon fuels. The deployment of blend 5 as replacement for R134a presented the most economically favorable performance, resulting in retrofitting cost savings, while higher costs are required for replacing R410A with blend 1. Moreover, blend 5 would not require modifications to current legislations or tax levels to ensure economic feasibility, as opposed to higher HFC utilization tax multiplier and installation of new taxing system on HFC emissions to ensure economic viability of blends 1–4.

The procedure presented here can be applied in the search for refrigerant blends for other cooling applications. Some restrictions imposed in this study can be relaxed or different weights can be given to the different KPIs, depending on the desired application. Overall, the strength of the methodology is based on the robust thermodynamic model to generate the required data for the design of the refrigeration cycles, without the need of further experiments. The next steps will be to experimentally test the validity of the proposed blends for the selected applications and their scale up, outside the scope of this work.

Credit roles

Carlos G. Albà (Conceptualization, Data Curation, Formal analysis, Investigation, Methodology, Visualization, Writing – original draft, Writing – review & editing); **Ismail I. I. Alkhatib** (Conceptualization, Methodology, Visualization, Writing – original draft, Writing – review & editing); **Fèlix Llovell** (Investigation, Formal analysis, Supervision, Writing – review & editing); **Lourdes F. Vega** (Conceptualization, Methodology, Project administration, Resources, Software, Funding acquisition, Supervision, Writing – review & editing).

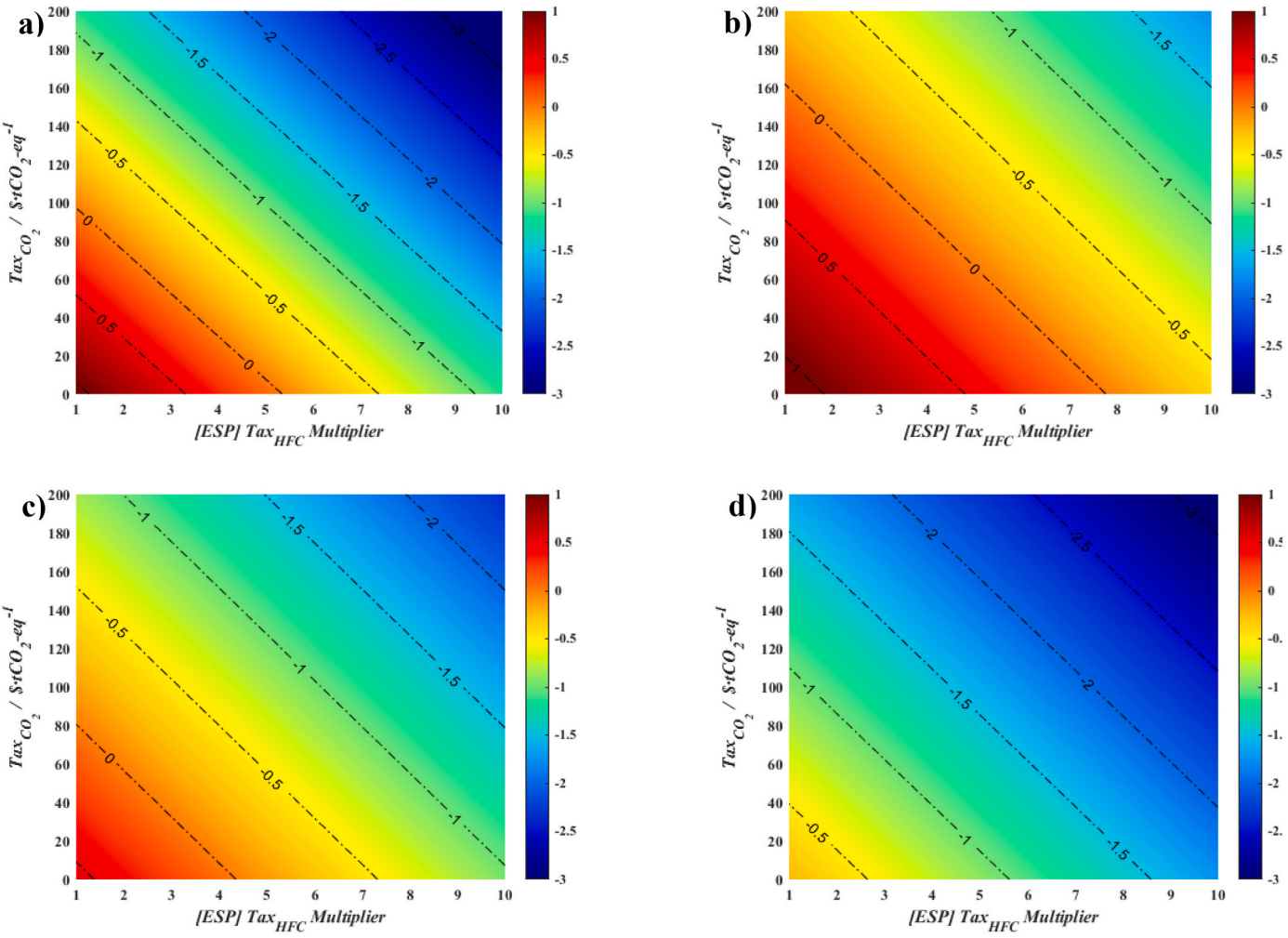

Fig. 12. Sensitivity analysis for change in TAC (in k$) of selected blends **a)** 1, **b)** 3, **c)** 4, and **d)** 5 based on HFC utilization tax multiplier on the Spanish framework (*x-axis*), and CO_2 equivalent tax for HFC emissions (*y-axis*). The dashed lines represent the cost variation compared to the baseline cost for EU in Fig. 10, with negative values representing increased savings, while positive values denote additional annual costs from the baseline cost.

Declaration of competing interest

The authors declare that they have no known competing financial interests or personal relationships that could have appeared to influence the work reported in this paper.

Data availability

Data will be made available on request.

Acknowledgments

This work was funded by Khalifa University through project RC2-2019-007 (RICH Center). Additional support was provided by the Spanish Ministry of Science and Innovation MCIN/AEI/10.13039/501100011033/under R + D + I project STOP-F-Gas (Ref: PID2019-108014RB-C21). C. G. Albà acknowledges a FI-SDUR fellowship from the Catalan Government. Computational resources from the RICH Center and the Almesbar HPC at the Research Computing department at Khalifa University are gratefully acknowledged.

Appendix A. Supplementary data

Supplementary data to this article can be found online at https://doi.org/10.1016/j.rser.2023.113806.

References

[1] Pathway to critical and formidable goal of net-zero emissions by 2050 is narrow but brings huge benefits, according to IEA special report - News - IEA 2021;1:1-224 https://www.iea.org/news/pathway-to-critical-and-formidable-goal-of-net-zero-emissions-by-2050-is-narrow-but-brings-huge-benefits (accessed February 18, 2022).

[2] Net zero: why is it necessary? | Energy & Climate Intelligence Unit 2022. https://eciu.net/analysis/briefings/net-zero/net-zero-why (accessed February 18, 2022).

[3] Falkner R. The Paris Agreement and the new logic of international climate politics. Int Aff 2016;92:1107–25. https://doi.org/10.1111/1468-2346.12708.

[4] Schulz M, Kourkoulas D. Regulation (EU) No 517/2014 of the European parliament and of the council of 16 april 2014 on fluorinated greenhouse gases and repealing regulation (EC) No 842/2006. Off J Eur Union 2014;2014:L150/195-230. https://doi.org/10.4271/1999-01-0874.

[5] UN Environment Ozone Secretariat. Ratification of the Kigali amendment. United Nations Environ Program; 2017.

[6] IPCC. Summary for policy makers. In: Masson-Delmotte V, Zhai P, Chen Y, Goldfarb L, Gomis MI, Matthews JBR, editors. Clim. Chang. 2021 phys. Sci. Basis. Cambridge University Press; 2021.

[7] Mota-Babiloni A, Navarro-Esbrí J, Makhnatch P, Molés F. Refrigerant R32 as lower GWP working fluid in residential air conditioning systems in Europe and the USA. Renew Sustain Energy Rev 2017;80:1031–42. https://doi.org/10.1016/j.rser.2017.05.216.

[8] Wu D, Hu B, Wang RZ. Vapor compression heat pumps with pure Low-GWP refrigerants. Renew Sustain Energy Rev 2021;138. https://doi.org/10.1016/j.rser.2020.110571.

[9] Maratou A. EU policy update-F-Gas Regulation, HFC taxes & fiscal incentives for natural refrigerants. Proceedings, Atmos Asia Conference, Toyo, Japan 2014; 1-40.

[10] Velders GJM, Fahey DW, Daniel JS, Andersen SO, McFarland M. Future atmospheric abundances and climate forcings from scenarios of global and regional hydrofluorocarbon (HFC) emissions. Atmos Environ 2015;123:200–9. https://doi.org/10.1016/j.atmosenv.2015.10.071.

[11] AIM Act | US EPA n.d. https://www.epa.gov/climate-hfcs-reduction/aim-act (accessed March 4, 2022).

[12] Kazakov A, McLinden MO, Frenkel M. Computational design of new refrigerant fluids based on environmental, safety, and thermodynamic characteristics. Ind Eng Chem Res 2012;51:12537–48. https://doi.org/10.1021/ie3016126.

[13] McLinden MO, Brown JS, Brignoli R, Kazakov AF, Domanski PA. Limited options for low-global-warming-potential refrigerants. Nat Commun 2017;8:1–9. https://doi.org/10.1038/ncomms14476.

[14] Albà CG, Alkhatib III, Llovell F, Vega LF. Assessment of low global warming potential refrigerants for drop-in replacement by connecting their molecular features to their performance. ACS Sustainable Chem Eng 2021;9:17034–48. https://doi.org/10.1021/acssuschemeng.1c05985.

[15] ASHRAE. ANSI/ASHRAE standard 34–2016 designation and safety classification of refrigerants. 2016.

[16] Wu X, Dang C, Xu S, Hihara E. State of the art on the flammability of hydrofluoroolefin (HFO) refrigerants. Int J Refrig 2019;108:209–23. https://doi.org/10.1016/j.ijrefrig.2019.08.025.

[17] Giménez-Prades P, Navarro-Esbrí J, Arpagaus C, Fernández-Moreno A, Mota-Babiloni A. Novel molecules as working fluids for refrigeration, heat pump and organic Rankine cycle systems. Renew Sustain Energy Rev 2022;167. https://doi.org/10.1016/j.rser.2022.112549.

[18] Abas N, Kalair AR, Khan N, Haider A, Saleem Z, Saleem MS. Natural and synthetic refrigerants, global warming: a review. Renew Sustain Energy Rev 2018;90:557–69. https://doi.org/10.1016/j.rser.2018.03.099.

[19] Bolaji BO, Huan Z. Ozone depletion and global warming: case for the use of natural refrigerant - a review. Renew Sustain Energy Rev 2013;18:49–54. https://doi.org/10.1016/j.rser.2012.10.008.

[20] Vuppaladadiyam AK, Antunes E, Vuppaladadiyam SSV, Baig ZT, Subiantoro A, Lei G, et al. Progress in the development and use of refrigerants and unintended environmental consequences. Sci Total Environ 2022;823:153670. https://doi.org/10.1016/j.scitotenv.2022.153670.

[21] Sanguri K, Ganguly K, Pandey A. Modelling the barriers to low global warming potential refrigerants adoption in developing countries: a case of Indian refrigeration industry. J Clean Prod 2021;280:124357. https://doi.org/10.1016/j.jclepro.2020.124357.

[22] Sovacool BK, Griffiths S, Kim J, Bazilian M. Climate change and industrial F-gases: a critical and systematic review of developments, sociotechnical systems and policy options for reducing synthetic greenhouse gas emissions. Renew Sustain Energy Rev 2021;141:110759. https://doi.org/10.1016/j.rser.2021.110759.

[23] Adamson KM, Walmsley TG, Carson JK, Chen Q, Schlosser F, Kong L, et al. High-temperature and transcritical heat pump cycles and advancements: a review. Renew Sustain Energy Rev 2022;167:112798. https://doi.org/10.1016/j.rser.2022.112798.

[24] Karagoz S, Yilmaz M, Comakli O, Ozyurt O. R134a and various mixtures of R22/R134a as an alternative to R22 in vapour compression heat pumps. Energy Convers Manag 2004;45:181–96. https://doi.org/10.1016/S0196-8904(03)00144-4.

[25] Fannou J-LC, Rousseau C, Lamarche L, Kajl S. A comparative performance study of a direct expansion geothermal evaporator using R410A and R407C as refrigerant alternatives to R22. Appl Therm Eng 2015;82:306–17. https://doi.org/10.1016/j.applthermaleng.2015.02.079.

[26] Heredia-Aricapa Y, Belman-Flores JM, Mota-Babiloni A, Serrano-Arellano J, García-Pabón JJ. Overview of low GWP mixtures for the replacement of HFC refrigerants: R134a, R404A and R410A. Int J Refrig 2020;111:113–23. https://doi.org/10.1016/j.ijrefrig.2019.11.012.

[27] Khalid Shaker Al-Sayyab A, Mota-Babiloni A, Navarro-Esbrí J. Novel compound waste heat-solar driven ejector-compression heat pump for simultaneous cooling and heating using environmentally friendly refrigerants. Energy Convers Manag 2021;228. https://doi.org/10.1016/j.enconman.2020.113703.

[28] Mota-Babiloni A, Belman-Flores JM, Makhnatch P, Navarro-Esbrí J, Barroso-Maldonado JM. Experimental exergy analysis of R513A to replace R134a in a small capacity refrigeration system. Energy 2018;162:99–110. https://doi.org/10.1016/j.energy.2018.08.028.

[29] Halon T, Gil B, Zajaczkowski B. Comparative investigation of low-GWP binary and ternary blends as potential replacements of HFC refrigerants for air conditioning systems. Appl Therm Eng 2022;210:118354. https://doi.org/10.1016/j.applthermaleng.2022.118354.

[30] Bamorovat Abadi G, Kim KC. Investigation of organic Rankine cycles with zeotropic mixtures as a working fluid: advantages and issues. Renew Sustain Energy Rev 2017;73:1000–13. https://doi.org/10.1016/j.rser.2017.02.020.

[31] Llopis R, Sánchez D, Cabello R, Catalán-Gil J, Nebot-Andrés L. Experimental analysis of R-450A and R-513A as replacements of R- 134a and R-507A in a medium temperature commercial refrigeration system. Int J Refrig 2017;84:52–66. https://doi.org/10.1016/j.ijrefrig.2017.08.022.

[32] Makhnatch P, Mota-Babiloni A, Khodabandeh R. Experimental study of R450A drop-in performance in an r134a small capacity refrigeration unit. Int J Refrig 2017;84:26–35. https://doi.org/10.1016/j.ijrefrig.2017.08.010.

[33] Mota-Babiloni A, Navarro-Esbrí J, Barragán-Cervera A, Molés F, Peris B. Drop-in analysis of an internal heat exchanger in a vapour compression system using R1234ze(E) and R450A as alternatives for R134a. Energy 2015;90:1636–44. https://doi.org/10.1016/j.energy.2015.06.133.

[34] Aprea C, Greco A, Maiorino A. Comparative performance analysis of HFO1234ze/HFC134a binary mixtures working as a drop-in of HFC134a in a domestic refrigerator. Int J Refrig 2017;82:71–82. https://doi.org/10.1016/j.ijrefrig.2017.07.001.

[35] Aprea C, Greco A, Maiorino A. HFOs and their binary mixtures with HFC134a working as drop-in refrigerant in a household refrigerator: energy analysis and environmental impact assessment. Appl Therm Eng 2018;141:226–33. https://doi.org/10.1016/j.applthermaleng.2018.02.072.

[36] Harby K. Hydrocarbons and their mixtures as alternatives to environmental unfriendly halogenated refrigerants: an updated overview. Renew Sustain Energy Rev 2017;73:1247–64. https://doi.org/10.1016/j.rser.2017.02.039.

[37] Oruç V, Devecioğlu AG. Experimental investigation on the low-GWP HFC/HFO blends R454A and R454C in a R404A refrigeration system. Int J Refrig 2021;128:242–51. https://doi.org/10.1016/j.ijrefrig.2021.04.007.

[38] Mota-Babiloni A, Haro-Ortuño J, Navarro-Esbrí J, Barragán-Cervera Á. Experimental drop-in replacement of R404A for warm countries using the low GWP mixtures R454C and R455A. Int J Refrig 2018;91:136–45. https://doi.org/10.1016/j.ijrefrig.2018.05.018.

[39] Llopis R, Calleja-Anta D, Sánchez D, Nebot-Andrés L, Catalán-Gil J, Cabello R. R-454C, R-459B, R-457A and R-455A as low-GWP replacements of R-404A: experimental evaluation and optimization. Int J Refrig 2019;106:133–43. https://doi.org/10.1016/j.ijrefrig.2019.06.013.

[40] Thu K, Takezato K, Takata N, Miyazaki T, Higashi Y. Drop-in experiments and exergy assessment of HFC-32/HFO-1234yf/R744 mixture with GWP below 150 for domestic heat pumps. Int J Refrig 2021;121:289–301. https://doi.org/10.1016/j.ijrefrig.2020.10.009.

[41] Bell IH, Domanski PA, McLinden MO, Linteris GT. The hunt for nonflammable refrigerant blends to replace R-134a. Int J Refrig 2019;104:484–95. https://doi.org/10.1016/j.ijrefrig.2019.05.035.

[42] Mastrullo R, Mauro AW, Napoli G, Pelella F, Viscito L. Flow boiling of azeotropic and non-azeotropic mixtures. Effect of the glide temperature difference on the nucleate boiling contribution: assessment of methods. J Phys Conf Ser 2020;1599:012053. https://doi.org/10.1088/1742-6596/1599/1/012053.

[43] Zhao Y, Li Z, Zhang X, Wang X, Dong X, Gao B, et al. Azeotropic refrigerants and its application in vapor compression refrigeration cycle. Int J Refrig 2019;108:1–13. https://doi.org/10.1016/j.ijrefrig.2019.08.024.

[44] Makhnatch P, Mota-Babiloni A, Khodabandeh R. The effect of temperature glide on the performance of refrigeration systems. In: 5th IIR int conf thermophys prop transf process refrig seoul; 2017. https://doi.org/10.18462/iir.tptpr.2017.0059.

[45] Didion DA, Bivens DB. Role of refrigerant mixtures as alternatives to CFCs. Int J Refrig 1990;13:163–75. https://doi.org/10.1016/0140-7007(90)90071-4.

[46] Kasaeian A, Hosseini SM, Sheikhpour M, Mahian O, Yan WM, Wongwises S. Applications of eco-friendly refrigerants and nanorefrigerants: a review. Renew Sustain Energy Rev 2018;96:91–9. https://doi.org/10.1016/j.rser.2018.07.033.

[47] Bell IH, Riccardi D, Bazyleva A, McLinden MO. Survey of data and models for refrigerant mixtures containing halogenated olefins. J Chem Eng Data 2021;66:2335–54. https://doi.org/10.1021/acs.jced.1c00192.

[48] Fernández-Moreno A, Mota-Babiloni A, Giménez-Prades P, Navarro-Esbrí J. Optimal refrigerant mixture in single-stage high-temperature heat pumps based on a multiparameter evaluation. Sustain Energy Technol Assessments 2022;52:101989. https://doi.org/10.1016/j.seta.2022.101989.

[49] Aprea C, Greco A, Maiorino A. HFOs and their binary mixtures with HFC134a working as drop-in refrigerant in a household refrigerator: energy analysis and environmental impact assessment. Appl Therm Eng 2018;141:226–33. https://doi.org/10.1016/j.applthermaleng.2018.02.072.

[50] Arami-Niya A, Xiao X, Al Ghafri SZS, Jiao F, Khamphasith M, Sadeghi Pouya E, et al. Measurement and modelling of the thermodynamic properties of carbon dioxide mixtures with HFO-1234yf, HFC-125, HFC-134a, and HFC-32: vapour-liquid equilibrium, density, and heat capacity. Int J Refrig 2020;118:514–28. https://doi.org/10.1016/j.ijrefrig.2020.05.009.

[51] Mickoleit E, Breitkopf C, Jäger A. Influence of equations of state and mixture models on the design of a refrigeration process. Int J Refrig 2021;121:193–205. https://doi.org/10.1016/j.ijrefrig.2020.10.017.

[52] Lemmon EW, Huber ML, McLinden MO. NIST reference fluid thermodynamic and transport properties — REFPROP, version 9.0. Gaithersburg, MD: National Institute of Standards and Technology; 2013.

[53] Chapman WG, Gubbins KE, Jackson G, Radosz M. SAFT: equation-of-state solution model for associating fluids. Fluid Phase Equil 1989;52:31–8. https://doi.org/10.1016/0378-3812(89)80308-5.

[54] Polishuk I, Chiko A, Cea-Klapp E, Garrido JM. Implementation of CP-PC-SAFT and CS-SAFT-VR-Mie for predicting the thermodynamic properties of C1-C3Halocarbon systems. II. Inter-relation between solubilities in ionic liquids, their pressure, volume, and temperature, and critical constants. Ind Eng Chem Res 2021;60:13084–93. https://doi.org/10.1021/acs.iecr.1c02720.

[55] Galindo A, Gil-Villegas A, Whitehead PJ, Jackson G, Burgess AN. Prediction of phase equilibria for refrigerant mixtures of difluoromethane (HFC-32), 1,1,1,2-tetrafluoroethane (HFC-134a), and pentafluoroethane (HFC-125a) using SAFT-VR. J Phys Chem B 1998;102:7632–9. https://doi.org/10.1021/jp9809437.

[56] Lampe M, Stavrou M, Schilling J, Sauer E, Gross J, Bardow A. Computer-aided molecular design in the continuous-molecular targeting framework using group-contribution PC-SAFT. Comput Chem Eng 2015;81:278–87. https://doi.org/10.1016/j.compchemeng.2015.04.008.

[57] Vilaseca O, Llovell F, Yustos J, Marcos RM, Vega LF. Phase equilibria, surface tensions and heat capacities of hydrofluorocarbons and their mixtures including the critical region. J Supercrit Fluids 2010;55:755–68. https://doi.org/10.1016/j.supflu.2010.10.015.

[58] Li Y, Fouad WA, Vega LF. Interfacial anomaly in low global warming potential refrigerant blends as predicted by molecular dynamics simulations. Phys Chem Chem Phys 2019;21:22092–102. https://doi.org/10.1039/c9cp03231b.

[59] Wang J, Chen D, Zhu L. Integrated working fluids and process optimization for refrigeration systems using polar PC-SAFT. Ind Eng Chem Res 2021;60:17640–9. https://doi.org/10.1021/ACS.IECR.1C03624/SUPPL_FILE/IE1C03624_SI_001.PDF.

[60] Avendaño C, Lafitte T, Adjiman CS, Galindo A, Müller EA, Jackson G. SAFT-γ force field for the simulation of molecular fluids: 2. Coarse-grained models of greenhouse gases, refrigerants, and long alkanes. J Phys Chem B 2013;117:2717–33. https://doi.org/10.1021/jp306442b.

[61] Swaminathan S, Visco DP. Thermodynamic modeling of refrigerants using the statistical associating fluid theory with variable range. 1. Pure components. Ind Eng Chem Res 2005;44:4798–805. https://doi.org/10.1021/ie048863e.

[62] Fouad WA, Vega LF. On the anomalous composition dependence of viscosity and surface tension in refrigerant blends. J Mol Liq 2018;268:190–200. https://doi.org/10.1016/j.molliq.2018.07.056.

[63] Fouad WA, Vega LF. The phase and interfacial properties of azeotropic refrigerants: the prediction of aneotropes from molecular theory. Phys Chem Chem Phys 2017;19:8977–88. https://doi.org/10.1039/c6cp08031f.

[64] Fouad WA. Thermal conductivity of pure fluids and multicomponent mixtures using residual entropy scaling with PC-SAFT - application to refrigerant blends. J Chem Eng Data 2020;65:5688–97. https://doi.org/10.1021/acs.jced.0c00682.

[65] Vinš V, Aminian A, Celný D, Součková M, Klomfar J, Čenský M, et al. Surface tension and density of dielectric heat transfer fluids of HFE type-experimental data at 0.1 MPa and modeling with PC-SAFT equation of state and density gradient theory. Int J Refrig 2021;131:956–69. https://doi.org/10.1016/j.ijrefrig.2021.06.029.

[66] Albà CG, Vega LF, Llovell F. A consistent thermodynamic molecular model of n-hydrofluoroolefins and blends for refrigeration applications. Int J Refrig 2020;113:145–55. https://doi.org/10.1016/j.ijrefrig.2020.01.008.

[67] Polishuk I, Assor E, Cohen N, Potievsky R. Implementation of PC-SAFT and SAFT + Cubic for modeling thermodynamic properties of haloalkanes. II. 7 Haloethanes and their mixtures. Int J Refrig 2013;36:980–91. https://doi.org/10.1016/j.ijrefrig.2012.10.034.

[68] Blas FJ, Vega LF. Thermodynamic behaviour of homonuclear and heteronuclear Lennard-Jones chains with association sites from simulation and theory. Mol Phys 1997;92:135–50. https://doi.org/10.1080/002689797170707.

[69] Alkhatib III, Pereira LMC, Torne J, Vega LF. Polar soft-SAFT: theory and comparison with molecular simulations and experimental data of pure polar fluids. Phys Chem Chem Phys 2020;22:13171–91. https://doi.org/10.1039/d0cp00846j.

[70] Alkhatib III, Albà CG, Darwish AS, Llovell F, Vega LF. Searching for sustainable refrigerants by bridging molecular modeling with machine learning. Ind Eng Chem Res 2022;61:7414–29. https://doi.org/10.1021/acs.iecr.2c00719.

[71] Johnson JK, Zollwef JA, Gubbins KE. The Lennard-Jones equation of state revisited. Mol Phys 1993;78:591–618. https://doi.org/10.1080/00268979300100411.

[72] Chapman WG, Gubbins KE, Jackson G, Radosz M. SAFT: equation-of-state solution model for associating fluids. Fluid Phase Equil 1989;52:31–8. https://doi.org/10.1016/0378-3812(89)80308-5.

[73] Chapman WG, Gubbins KE, Jackson G, Radosz M. New reference equation of state for associating liquids. Ind Eng Chem Res 1990;29:1709–21. https://doi.org/10.1021/ie00104a021.

[74] Wertheim MS. Fluids with highly directional attractive forces. IV. Equilibrium polymerization. J Stat Phys 1986;42:477–92. https://doi.org/10.1007/BF01127722.

[75] Wertheim MS. Fluids with highly directional attractive forces . III. Multiple attraction sites. J Stat Phys 1986;42:459–76. https://doi.org/10.1007/BF01127721.

[76] Wertheim MS. Fluids with highly directional attractive forces. II. Thermodynamic perturbation theory and integral equations. J Stat Phys 1984;35:35–47. https://doi.org/10.1007/BF01017363.

[77] Wertheim MS. Fluids with highly directional attractive forces. I. Statistical thermodynamics. J Stat Phys 1984;35:19–34. https://doi.org/10.1007/BF01017362.

[78] Gubbins KE, Twu CH. Thermodynamics of polyatomic fluid mixtures-I: theory. Chem Eng Sci 1978;33:863–78. https://doi.org/10.1016/0009-2509(78)85176-8.

[79] Twu CH, Gubbins KE. Thermodynamics of polyatomic fluid mixtures—II: polar, quadrupolar and octopolar molecules. Chem Eng Sci 1978;33:879–87. https://doi.org/10.1016/0009-2509(78)85177-x.

[80] Jog PK, Chapman WG. Application of Wertheim's thermodynamic perturbation theory to dipolar hard sphere chains. Mol Phys 1999;97:307–19. https://doi.org/10.1080/00268970601076467.

[81] Jog PK, Sauer SG, Blaesing J, Chapman WG. Application of dipolar chain theory to the phase behavior of polar fluids and mixtures. Ind Eng Chem Res 2001;40:4641–8. https://doi.org/10.1021/ie010264+.

[82] Stell G, Rasaiah JC, Narang H. Thermodynamic perturbation theory for simple polar fluids. II. Mol Phys 1974;27:1393–414. https://doi.org/10.1080/00268977400101181.

[83] Luckas M, Lucas K, Deiters U, Gubbins KE. Integrals over pair- and triplet-correlation functions for the Lennard-Jones (12-6)-fluid. Mol Phys 1986;57:241–53. https://doi.org/10.1080/00268978600100191.

[84] Alkhatib III, Vega LF. Quantifying the effect of polarity on the behavior of mixtures of n-alkanes with dipolar solvents using polar soft-SAFT. AIChE J 2020;67:e16649. https://doi.org/10.1002/aic.16649.

[85] Alkhatib III, Llovell F, Vega LF. Assessing the effect of impurities on the thermophysical properties of methane-based energy systems using polar soft-SAFT. Fluid Phase Equil 2021;527:112841. https://doi.org/10.1016/j.fluid.2020.112841.

[86] Alkhatib III, Vega LF. Quantifying the effect of polar interactions on the behavior of binary mixtures: phase, interfacial, and excess properties. J Chem Phys 2021;154:164503. https://doi.org/10.1063/5.0046034.

[87] Blas FJ, Vega LF. Prediction of binary and ternary diagrams using the statistical associating fluid theory (SAFT) equation of state. Ind Eng Chem Res 1998;37:660–74. https://doi.org/10.1021/ie970449+.

[88] Albà CG, Llovell F, Vega LF. Searching for suitable lubricants for low global warming potential refrigerant R513A using molecular-based models: solubility and performance in refrigeration cycles. Int J Refrig 2021;128:252–63. https://doi.org/10.1016/j.ijrefrig.2021.04.010.

[89] Lim JS, Park JY, Lee BG. Vapor-liquid equilibria of CFC alternative refrigerant mixtures: trifluoromethane (HFC-23) + difluoromethane (HFC-32), trifluoromethane (HFC-23) + pentafluoroethane (HFC-125), and pentafluoroethane (HFC-125) + 1,1-difluoroethane (HFC-152a). Int J Thermophys 2000;21:1339–49. https://doi.org/10.1023/A:1006653309953.

[90] Qin Y, Li N, Zhang H, Liu B. Energy and exergy analysis of a Linde-Hampson refrigeration system using R170, R41 and R1132a as low-GWP refrigerant blend components to replace R23. Energy 2021;229:120645. https://doi.org/10.1016/j.energy.2021.120645.

[91] Raabe G. Molecular simulation data for the vapor-liquid phase equilibria of binary mixtures of HFO-1123 with R-32, R-1234yf, R-1234ze(E), R-134a and CO2 and their modelling by the PCP-SAFT equation of state. Data Brief 2019;25:104014. https://doi.org/10.1016/j.dib.2019.104014.

[92] Meng X, Hu X, Yang T, Wu J. Vapor liquid equilibria for binary mixtures of difluoromethane (R32) + fluoroethane (R161) and fluoroethane (R161) + trans-1,3,3,3-tetrafluoropropene (R1234ze(E)). J Chem Thermodyn 2018;118:43–50. https://doi.org/10.1016/j.jct.2017.10.015.

[93] Lee BG, Park JY, Lim JS, Cho SY, Park KY. Phase equilibria of chlorofluorocarbon alternative refrigerant mixtures. J Chem Eng Data 1999;44:190–2. https://doi.org/10.1021/je980180g.

[94] Hu X, Yang T, Meng X, Bi S, Wu J. Vapor liquid equilibrium measurements for difluoromethane (R32) + 2,3,3,3-tetrafluoroprop-1-ene (R1234yf) and fluoroethane (R161) + 2,3,3,3-tetrafluoroprop-1-ene (R1234yf). Fluid Phase Equil 2017;438:10–7. https://doi.org/10.1016/j.fluid.2017.01.024.

[95] Yang Z, Valtz A, Coquelet C, Wu J, Lu J. Experimental measurement and modelling of vapor-liquid equilibrium for 3,3,3- Trifluoropropene (R1243zf) and trans-1,3,3,3-Tetrafluoropropene (R1234ze(E)) binary system. Int J Refrig 2020;120:137–49. https://doi.org/10.1016/j.ijrefrig.2020.08.016.

[96] Kou L, Yang Z, Tang X, Zhang W, Lu J. Experimental measurements and correlation of isothermal vapor-liquid equilibria for HFC-32 + HFO-1234ze (E) and HFC-134a + HFO-1234ze (E) binary systems. J Chem Thermodyn 2019;139:105798. https://doi.org/10.1016/j.jct.2019.04.020.

[97] Han X, Ye G, Fang Y, Guo Z, Ni H, Zhuang Y, et al. Experimental investigation of vapor-liquid equilibrium for 2,3,3,3-tetrafluoropropene (HFO-1234yf) + trans-1,3,3,3-tetrafluoropropene (HFO-1234ze(E)) at Temperatures from 284 to 334 K. J Chem Eng Data 2021;66:1741–53. https://doi.org/10.1021/acs.jced.0c01033.

[98] Madani H, Valtz A, Zhang F, El Abbadi J, Houriez C, Paricaud P, et al. Isothermal vapor-liquid equilibrium data for the trifluoromethane (R23) + 2,3,3,3-tetrafluoroprop-1-ene (R1234yf) system at temperatures from 254 to 348 K. Fluid Phase Equil 2016;415:158–65. https://doi.org/10.1016/j.fluid.2016.02.005.

[99] Abbadi J El, Coquelet C, Valtz A, Houriez C. Experimental measurements and modelling of vapour−liquid equilibria for four mixtures of 2,3,3,3−tetrafluoropropene (R1234yf) with 1,1,1,2−tetrafluoroethane (R134a) or 1,1−difluoroethane (R152a) or trans−1−chloro−3,3,3−trifluoropropene (R1233zd(E)) or 2−c. Int J Refrig 2022;140:172–85. https://doi.org/10.1016/j.ijrefrig.2022.05.006.

[100] Bobbo S, Camporese R, Stryjek R. Vapor-liquid equilibria for difluoromethane (R32) + and pentafluoroethane (R125) + 1,1,1,3,3,3-hexafluoropropane (R236fa) at 303.2 and 323.3 K. J Chem Eng Data 1999;44:349–52. https://doi.org/10.1021/je980195e.

[101] Park JY, Lim JS, Lee BG, Lee YW. Phase equilibria of CFC alternative refrigerant mixtures: 1, 1, 1, 2, 3, 3, 3-heptafluoropropane (HFC-227ea)+ difluoromethane (HFC-32),+ 1, 1, 1, 2-tetrafluoroethane. Int J Thermophys 2001;22:901–17. https://doi.org/10.1023/A:1010735318011.

[102] Lim JS, Park KH, Lee BG. Phase equilibria of HFC mixtures: binary mixtures of trifluoromethane + 1,1-difluoroethane and trifluoromethane + 1,1,1-trifluoroethane at 283.15 and 293.15 K. J Chem Eng Data 2002;47:582–6. https://doi.org/10.1021/je0102311.

[103] Peng S, Wang E, Yang Z, Duan Y. Vapor-liquid equilibrium measurements for the binary mixtures of 1,1-difluoroethane (R152a) with trans-1,3,3,3-tetrafluoropropene (R1234ze(E)) and 3,3,3-trifluoropropene (R1243zf). Fluid Phase Equil 2022:558. https://doi.org/10.1016/j.fluid.2022.113470.

[104] Cui XL, Chen GM, Han XH, Li CS. Vapor−Liquid equilibria for the trifluoromethane + 1,1,1,2-tetrafluoroethane system. J Chem Eng Data 2006;51:1927. https://doi.org/10.1021/je0602622. –30.

[105] Yang T, Hu X, Meng X, Wu J. Vapor–liquid equilibria for the binary and ternary systems of difluoromethane (R32), 1,1-difluoroethane (R152a), and 2,3,3,3-Tetrafluoroprop-1-ene (R1234yf). J Chem Eng Data 2018;63:771–80. https://doi.org/10.1021/acs.jced.7b00950.

[106] Yang Z, Gong M, Guo H, Dong X, Wu J. Phase equilibrium for the binary mixture of {1,1-difluoroethane (R152a)+trans-1,3,3,3-tetrafluoropropene (R1234ze (E))} at various temperatures from 258.150 to 288.150K. Fluid Phase Equil 2013;355:99–103. https://doi.org/10.1016/j.fluid.2013.06.017.

[107] Lim JS, Park KH, Lee BG, Kim JD. Phase equilibria of CFC alternative refrigerant mixtures. Binary systems of trifluoromethane (HFC-23) + 1,1,1,2-tetrafluoroethane (HFC-134a) and trifluoromethane (HFC-23) + 1,1,1,2,3,3,3-heptafluoropropane (HFC-227ea) at 283.15 and 293.15 K. J Chem Eng Data 2001;46:1580–3. https://doi.org/10.1021/je010103c.

[108] Yao X, Ding L, Dong X, Zhao Y, Wang X, Shen J, et al. Experimental measurement of vapor-liquid equilibrium for 3,3,3-trifluoropropene(R1243zf) + 1,1,1,2-tetrafluoroethane(R134a) at temperatures from 243.150 to 293.150 K. Int J Refrig 2020;120:97–103. https://doi.org/10.1016/j.ijrefrig.2020.09.008.

[109] Dong X, Gong M, Zhang Y, Wu J. Vapor−Liquid equilibria of the fluoroethane (R161) + 1,1,1,2-tetrafluoroethane (R134a) system at various temperatures from (253.15 to 292.92) K. J Chem Eng Data 2008;53:2193–6. https://doi.org/10.1021/je800505y.

[110] Kamiaka T, Dang C, Hihara E. Vapor-liquid equilibrium measurements for binary mixtures of R1234yf with R32, R125, and R134a. Int J Refrig 2013;36:965–71. https://doi.org/10.1016/j.ijrefrig.2012.08.016.

[111] Han XH, Chen GM, Li CS, Qiao XG, Cui XL, Wang Q. Isothermal vapor - liquid equilibrium of (pentafluoroethane + fluoroethane) at temperatures between (265.15 and 303.15) K obtained with a recirculating still. J Chem Eng Data 2006;51:1232–5. https://doi.org/10.1021/je050539i.

[112] Wang Q, Xu YJ, Gao ZJ, Qiu Y, Min XW, Han XH, et al. Isothermal vapor-liquid equilibrium data for the binary mixture ethyl fluoride (HFC-161)+1,1,1,2,3,3,3-heptafluoroproane (HFC-227ea) over a temperature range from 253.15K to 313.15K. Fluid Phase Equil 2010;297:67–71. https://doi.org/10.1016/j.fluid.2010.06.006.

[113] Kleiber M. Vapor-liquid equilibria of binary refrigerant mixtures containing propylene or R134a. Fluid Phase Equil 1994;92:149–94. https://doi.org/10.1016/0378-3812(94)80046-4.

[114] Yang T, Hu X, Meng X, Wu J. Vapour-liquid equilibria for the binary systems of pentafluoroethane {(R125) + 2,3,3,3-tetrafluoroprop-1-ene (R1234yf)} and {trans-1,3,3,3-tetrafluoropropene R1234ze(E). J Chem Thermodyn 2020;150:106222. https://doi.org/10.1016/j.jct.2020.106222.

[115] Nishiumi H, Akita H, Akiyama S. High pressure vapor-liquid equilibria for the HFC125-HFC152a system. Kor J Chem Eng 1997;14:359–64. https://doi.org/10.1007/BF02707052.

[116] Li X, Pang Q, Liu J, Ning Q, He G. Isothermal vapour-liquid equilibrium data for environmentally friendly binary system {R1234ze(E) + R245fa. J Chem Thermodyn 2022;175. https://doi.org/10.1016/j.jct.2022.106894.

[117] Yang L, Gong M, Guo H, Dong X, Wu J. (Vapour + liquid) equilibrium data for the {1,1-difluoroethane (R152a) + 1,1,1,3,3-pentafluoropropane (R245fa)} system at temperatures from (323.150 to 353.150) K. J Chem Thermodyn 2015;91:414–9. https://doi.org/10.1016/j.jct.2015.08.024.

[118] Hu P, Chen LX, Zhu WB, Jia L, Chen ZS. Vapor-liquid equilibria for the binary system of 2,3,3,3-tetrafluoroprop-1-ene (HFO-1234yf)+1,1,1,2,3,3,3-heptafluoropropane (HFC-227ea). Fluid Phase Equil 2014;379:59–61. https://doi.org/10.1016/j.fluid.2014.07.014.

[119] Honeywell. SOLSTICE N15 (R-515B) technical data sheet. 2021.

[120] Kato R, Nishiumi H. Vapor–liquid equilibria and critical loci of binary and ternary systems composed of CH2F2, C2HF5 and C2H2F4. Fluid Phase Equil 2006;249:140–6. https://doi.org/10.1016/j.fluid.2006.07.017.

[121] Bobbo S, Fedele L, Scattolini M, Camporese R. Isothermal VLE measurements for the binary mixtures HFC-134a + HFC-245fa and HC-600a + HFC-245fa. Fluid Phase Equil 2001;185:255–64. https://doi.org/10.1016/S0378-3812(01)00475-7.

[122] Bobbo S, Stryjek R, Elvassore N, Bertucco A. A recirculation apparatus for vapor-liquid equilibrium measurements of refrigerants. Binary mixtures of R600a, R134a and R236fa. Fluid Phase Equil 1998;150:343–52. https://doi.org/10.1016/s0378-3812(98)00334-3.

[123] Bobbo S, Camporese R, Scalabrin G. Isothermal vapour-liquid equilibrium measurements for the binary mixtures HFC-125 + HFC-245fa and HC-290 + HFC-245fa. High Temp - High Press 2000;32:441–7. https://doi.org/10.1068/htwu123.

[124] Hou SX, Duan YY. Isothermal vapor-liquid equilibria for the pentafluoroethane + propane and pentafluoroethane + 1,1,1,2,3,3,3-heptafluoropropane systems. Fluid Phase Equil 2010;290:121–6. https://doi.org/10.1016/j.fluid.2009.09.008.

[125] Luo D, Mahmoud A, Cogswell F. Evaluation of low-GWP fluids for power generation with organic rankine cycle. Energy 2015;85:481–8. https://doi.org/10.1016/j.energy.2015.03.109.

[126] Pardo F, Zarca G, Urtiaga A. Effect of feed pressure and long-term separation performance of Pebax-ionic liquid membranes for the recovery of difluoromethane (R32) from refrigerant mixture R410A. J Membr Sci 2021;618:118744. https://doi.org/10.1016/j.memsci.2020.118744.

[127] Linteris GT, Bell IH, McLinden MO. An empirical model for refrigerant flammability based on molecular structure and thermodynamics. Int J Refrig 2019;104:144–50. https://doi.org/10.1016/j.ijrefrig.2019.05.006.

[128] Linteris G, Babushok V. Laminar burning velocity predictions for C1 and C2 hydrofluorocarbon refrigerants with air. J Fluor Chem 2020;230:109324. https://doi.org/10.1016/j.jfluchem.2019.05.002.

[129] Babushok VI, Burgess DR, Hegetschweiler MJ, Linteris GT. Flame propagation in the mixtures of O2/N2 oxidizer with fluorinated propene refrigerants (CH2CFCF3, CHFCHCF3, CH2CHCF3). Combust Sci Technol 2021;193:1949–72. https://doi.org/10.1080/00102202.2020.1720663.

[130] Ahamed J, Saidur R, Masjuki HH. A review on exergy analysis of vapor compression refrigeration system. Renew Sustain Energy Rev 2011;15:1593–600. https://doi.org/10.1016/j.rser.2010.11.039.

[131] Bayrakçi HC, Özgür AE. Energy and exergy analysis of vapor compression refrigeration system using pure hydrocarbon refrigerants. Int J Energy Res 2009;33:1070–5. https://doi.org/10.1002/er.1538.

[132] Gholamian E, Hanafizadeh P, Ahmadi P. Advanced exergy analysis of a carbon dioxide ammonia cascade refrigeration system. Appl Therm Eng 2018;137:689–99. https://doi.org/10.1016/j.applthermaleng.2018.03.055.

[133] Al-Sayyab AKS, Navarro-Esbrí J, Mota-Babiloni A. Energy, exergy, and environmental (3E) analysis of a compound ejector-heat pump with low GWP refrigerants for simultaneous data center cooling and district heating. Int J Refrig 2022;133:61–72. https://doi.org/10.1016/j.ijrefrig.2021.09.036.

[134] Gill J, Singh J, Ohunakin OS, Adelekan DS. Exergy analysis of vapor compression refrigeration system using R450A as a replacement of R134a. J Therm Anal Calorim 2019;136:857–72. https://doi.org/10.1007/s10973-018-7675-z.

[135] AIRAH. Methods of calculating total equivalent warming impact. TEWI); 2012. 2012.

[136] Parikhani T, Bahman A, Ziviani D, Bahman AM. Techno-economic analysis for two-stage vapor injected system techno-economic analysis for two-stage vapor injected system for heating applications for heating applications techno-economic analysis for two-stage vapor injected system for heating applicatio. Int Refrig Air Cond Conf 2021;2534:1–9.

[137] Mosaffa AH, Farshi LG, Infante Ferreira CA, Rosen MA. Exergoeconomic and environmental analyses of CO2/NH3 cascade refrigeration systems equipped with different types of flash tank intercoolers. Energy Convers Manag 2016;117:442–53. https://doi.org/10.1016/j.enconman.2016.03.053.

[138] Navidbakhsh M, Shirazi A, Sanaye S. Four E analysis and multi-objective optimization of an ice storage system incorporating PCM as the partial cold storage for air-conditioning applications. Appl Therm Eng 2013;58:30–41. https://doi.org/10.1016/j.applthermaleng.2013.04.002.

[139] Roy R, Mandal BK. Thermo-economic assessment and multi-objective optimization of vapour compression refrigeration system using low GWP refrigerants. In: 2019 8th int. Conf. Model. Simul. Appl. Optim. IEEE; 2019. p. 1–5. https://doi.org/10.1109/ICMSAO.2019.8880390.

[140] Turgut MS, Turgut OE. Comparative investigation and multi objective design optimization of R744/R717, R744/R134a and R744/R1234yf cascade rerfigeration systems. Heat Mass Transf Und Stoffuebertragung 2019;55:445–65. https://doi.org/10.1007/S00231-018-2435-Y/FIGURES/14.

[141] Estado J del. Ley 6/2018, de 3 de julio, de Presupuestos Generales del Estado para el año 2018. Boletín Of Del Estado; 2018. BOE-A-2018:66621–7354.

[142] Kim YJ, Simmrock KH. AZEOPERT: an expert system for the prediction of azeotrope formation—I. Binary azeotropes. Comput Chem Eng 1997;21:93–111. https://doi.org/10.1016/0098-1354(95)00249-9.

[143] Meng Z, Zhang H, Lei M, Qin Y, Qiu J. Performance of low GWP R1234yf/R134a mixture as a replacement for R134a in automotive air conditioning systems. Int J Heat Mass Tran 2018;116:362–70. https://doi.org/10.1016/j.ijheatmasstransfer.2017.09.049.

[144] Li G. Performance evaluation of low global warming potential working fluids as R134a alternatives for two-stage centrifugal chiller applications. Kor J Chem Eng 2021;38:1438–51. https://doi.org/10.1007/s11814-021-0785-5.

[145] Mota-Babiloni A, Mateu-Royo C, Navarro-Esbrí J, Barragán-Cervera Á. Experimental comparison of HFO-1234ze(E) and R-515B to replace HFC-134a in heat pump water heaters and moderately high temperature heat pumps. Appl Therm Eng 2021;196:117256. https://doi.org/10.1016/j.applthermaleng.2021.117256.

[146] Askar E, Schröder V, Schmid T, Schwarze M. Explosion characteristics of mildly flammable refrigerants ignited with high-energy ignition sources in closed systems. Int J Refrig 2018;90:249–56. https://doi.org/10.1016/j.ijrefrig.2018.04.009.

[147] Mota-Babiloni A, Navarro-Esbrí J, Makhnatch P, Molés F. Refrigerant R32 as lower GWP working fluid in residential air conditioning systems in Europe and the USA. Renew Sustain Energy Rev 2017;80:1031–42. https://doi.org/10.1016/j.rser.2017.05.216.

[148] Mota-Babiloni A, Makhnatch P, Khodabandeh R, Navarro-Esbrí J. Experimental assessment of R134a and its lower GWP alternative R513A. Int J Refrig 2017;74:682–8. https://doi.org/10.1016/j.ijrefrig.2016.11.021.

[149] Makhnatch P, Mota-Babiloni A, López-Belchí A, Khodabandeh R. R450A and R513A as lower GWP mixtures for high ambient temperature countries: experimental comparison with R134a. Energy 2019;166:223–35. https://doi.org/10.1016/j.energy.2018.09.001.

[150] Booten C, Nicholson S, Mann M, Abdelaziz O. Refrigerants: market trends and supply chain assessment. 2020. Technical Report NREL/TP-5500-70207.

[151] Ohm T, Myung S, Jang W, Yu S. A comparison of refrigerant management policies and suggestions for improvement in South Korea. J Mater Cycles Waste Manag 2017;19:631–44. https://doi.org/10.1007/s10163-015-0455-y.

[152] Arpagaus C, Bless F, Uhlmann M, Schiffmann J, Bertsch SS. High temperature heat pumps: market overview, state of the art, research status, refrigerants, and application potentials. Energy 2018;152:985–1010. https://doi.org/10.1016/j.energy.2018.03.166.

[153] Chen X, Liang K, Li Z, Zhao Y, Xu J, Jiang H. Experimental assessment of alternative low global warming potential refrigerants for automotive air conditioners application. Case Stud Therm Eng 2020;22:100800. https://doi.org/10.1016/j.csite.2020.100800.